# Age, Correlation, and Lithostratigraphic Revision of the Upper Cretaceous (Campanian) Judith River Formation in Its Type Area (North-Central Montana), with a Comparison of Low- and High-Accommodation Alluvial Records

*Raymond R. Rogers,[1,*] Susan M. Kidwell,[2] Alan L. Deino,[3] James P. Mitchell,[4] Kenneth Nelson,[1] and Jeffrey T. Thole[1]*

*1. Geology Department, Macalester College, 1600 Grand Avenue, Saint Paul, Minnesota 55105, USA; 2. Department of the Geophysical Sciences, University of Chicago, 5734 South Ellis Avenue, Chicago, Illinois 60637, USA; 3. Berkeley Geochronology Center, 2455 Ridge Road, Berkeley, California 94709, USA; 4. Bureau of Land Management, Lewistown Field Office, 920 NE Main Street, Lewistown, Montana 59457, USA*

**ABSTRACT**

Despite long-standing significance in the annals of North American stratigraphy and paleontology, key aspects of the Upper Cretaceous Judith River Formation remain poorly understood. We re-evaluate Judith River stratigraphy and propose new reference sections that both document the range of lithologies present in the type area in north-central Montana and reveal dramatic changes in facies architecture, fossil content, and rock accumulation rates that can be mapped throughout the type area and into the plains of southern Alberta and Saskatchewan. One section spans the basal contact of the Judith River Formation with marine shales of the underlying Claggett Formation. This contact, which lies along the base of the Parkman Sandstone Member of the Judith River Formation, is erosional and consistent with an episode of forced regression, contrary to previous descriptions. A second reference section spans the entire Judith River Formation. This complete section hosts a lithologic discontinuity, herein referred to as the mid-Judith discontinuity, that reflects a regional reorganization of terrestrial and marine depositional systems associated with a turnaround from regressive to transgressive deposition. The mid-Judith discontinuity correlates with the base of three backstepping marine sequences in the eastern sector of the type area and is thus interpreted as the terrestrial expression of a maximum regressive surface. This mid-Judith discontinuity defines the boundary between the new McClelland Ferry and overlying Coal Ridge Members of the Judith River Formation. The shallow marine sandstones that form the backstepping sequences represent the leading edge of the Bearpaw transgression in this region and are formalized as the new Woodhawk Member of the Judith River Formation in a third reference section. New $^{40}Ar/^{39}Ar$ ages indicate (1) that the mid-Judith discontinuity formed ~76.2 Ma, coincident with the onset of the Bearpaw transgression in central Montana; and (2) that the Bearpaw Sea had advanced westward beyond the Judith River type area by ~75.2 Ma, on the basis of the dating of a bentonite bed at the base of the Bearpaw Formation. These new ages also provide more confident age control for important vertebrate fossil occurrences in the Judith River Formation. Facies analysis across the mid-Judith discontinuity reveals how alluvial systems respond to regional base-level rise, which is implicit with the increase in rock accumulation rates and marine transgression. With the increase in accommodation signaled by the mid-Judith discontinuity, the alluvial system shifted in dominance from fluvial channel to overbank deposits, with greater tidal influence in channel sands, more hydromorphic and carbonaceous overbank deposits, and a higher frequency of bentonites and skeletal concentrations, suggesting higher preservation rates. These features, along with the appearance of extraformational pebbles above the discontinuity, are consistent with an upstream tectonic explanation for the addition of accommodation.

**Online enhancements:** supplementary table.

## Introduction

The Upper Cretaceous (Campanian) Judith River Formation is widely exposed in Montana and constitutes the distal part of one of the major eastward-thinning clastic tongues of the Cretaceous section in the Western Interior Foreland Basin (Weimer 1960; Gill and Cobban 1973; Kauffman 1977; figs. 1, 2). The type area of the Judith River Formation lies in the Upper Missouri River Breaks National Monument (UMRBNM), a vast region of sparsely vegetated cou-

Manuscript received February 16, 2015; accepted September 18, 2015; electronically published February 17, 2016.

* Author for correspondence; e-mail: rogers@macalester.edu.

[The Journal of Geology, 2016, volume 124, p. 99–135]  0022-1376/2016/12401-0005$15.00. DOI: 10.1086/684289

lees and badlands in the Missouri River drainage in north-central Montana. Government-sponsored expeditions made frequent forays into the type area during the mid- to late nineteenth and early twentieth centuries, and stratigraphic research on the age and correlation of the formation was instrumental in resolving the basic stratigraphy of the Western Interior Cretaceous section (e.g., Meek and Hayden 1856, 1857; Hayden 1857, 1871; Dawson 1875; Meek 1876; Hatcher 1903*a*,1903*b*; Hatcher and Stanton 1903; Stanton and Hatcher 1905; Bowen 1915; reviewed in Waage 1975). The Judith River Formation is also significant to the history of vertebrate paleontology, with some of the first skeletal remains of dinosaurs described from North America recovered from it near the confluence of the Judith and Missouri Rivers (Leidy 1856, 1860; Cope 1876, 1877; Sternberg 1914). The formation has continued to be a major source of paleobiological data to the present day (e.g., Cope 1871, 1877; Sahni 1972; Tschudy

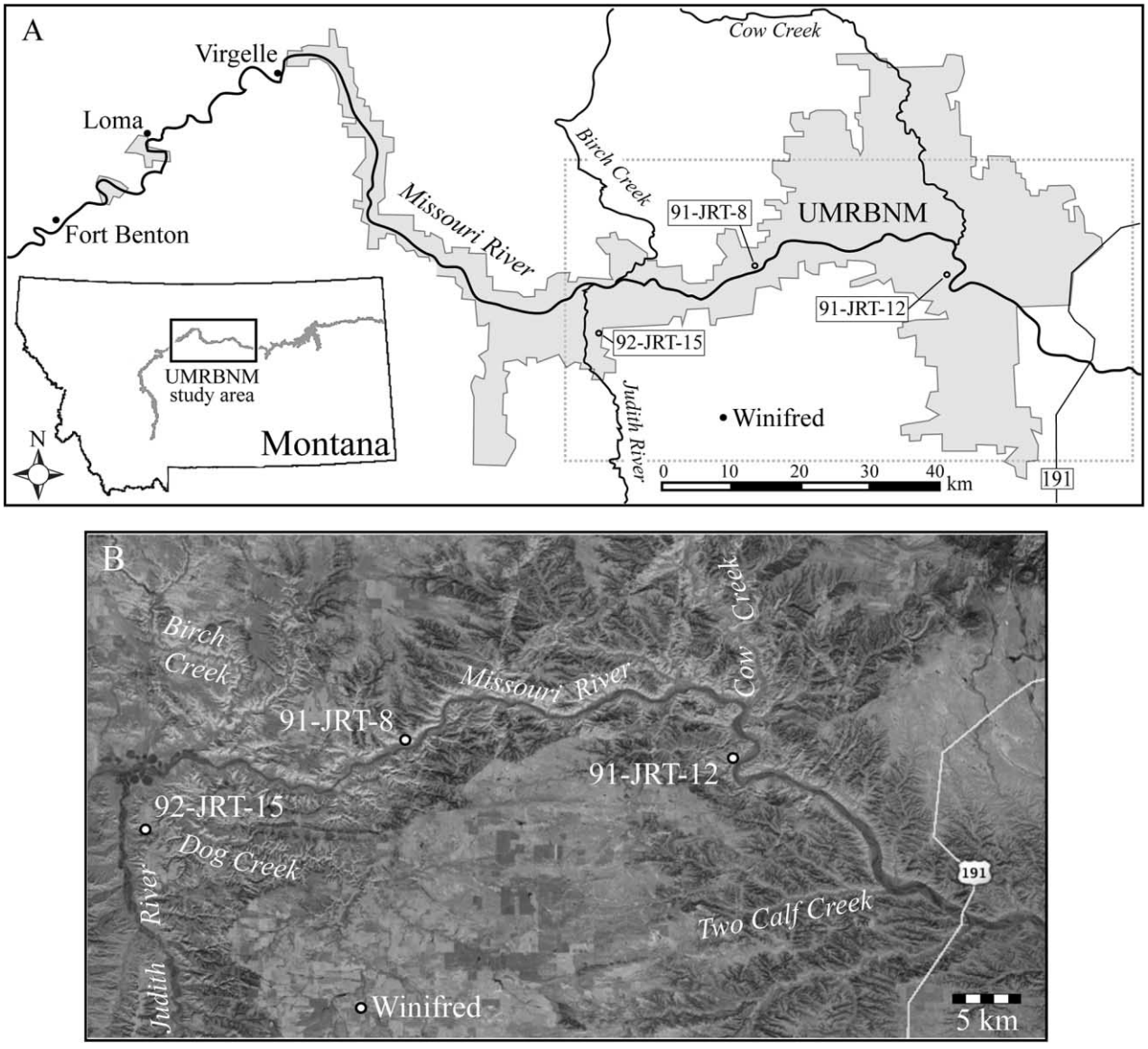


**Figure 1.** Judith River Formation study area. *A*, Map of north-central Montana showing boundaries of Upper Missouri River Breaks National Monument (UMRBNM; gray). Dotted box delimits region that includes the Judith River Formation type area. *B*, Satellite image of Judith River Formation type area along drainage of Missouri River in UMRBNM. Locations of three new reference sections (92-JRT-15, 91-JRT-8, 91-JRT-12) are indicated. Modified from Google Earth. A color version of this figure is available online.

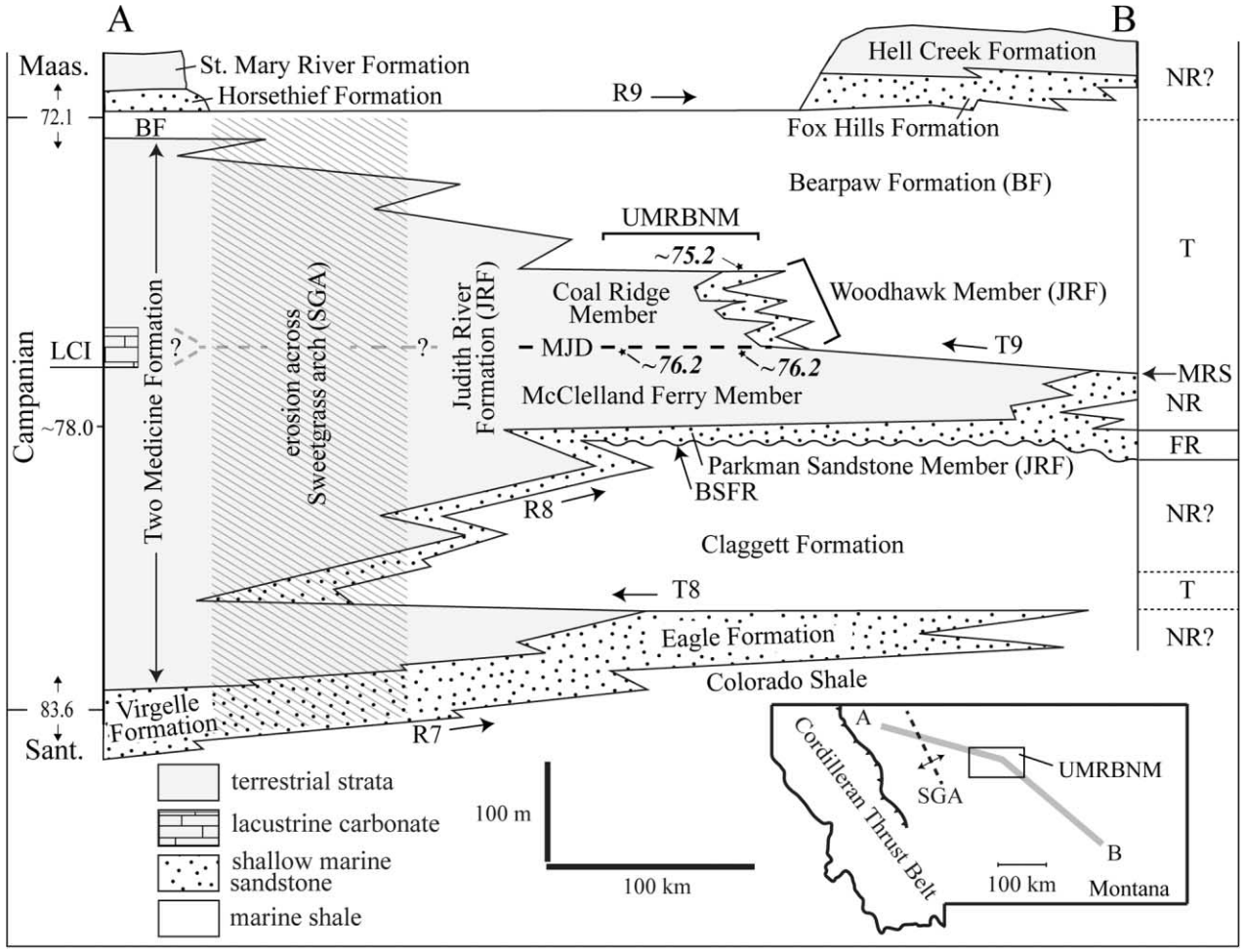


**Figure 2.** Schematic cross section of Upper Cretaceous strata in Montana (modified from Gill and Cobban 1973). The Judith River Formation correlates to the west with terrestrial deposits of the middle and upper Two Medicine Formation and is bounded above and below by marine shales of the Bearpaw and Claggett Formations. Regional regressive (R7, R8, R9) and transgressive (T8, T9) phases of deposition are from Kauffman (1977). The type area of the Judith River Formation is located in the Upper Missouri River Breaks National Monument (UMRBNM). The new Woodhawk Member crops out in the eastern sector of the type area and consists of three backstepping fourth-order sequences that accumulated during the Bearpaw transgression. The mid-Judith discontinuity (MJD) correlates with the base of the Woodhawk Member and separates the new McClelland Ferry Member below from the new Coal Ridge Member above. The erosional base of the Parkman Sandstone Member of the Judith River Formation in the UMRBNM reflects an episode of forced regression (FR), capping the normal regressive (NR) deposits of the upper Claggett Formation. The downward trajectory of the Parkman Sandstone Member at the eastern edge of the diagram is based on the original facies reconstruction of Gill and Cobban (1973) but is here interpreted as tracking a basal surface of forced regression (BSFR). The sandstone-rich alluvial McClelland Ferry Member was deposited during normal regression under conditions of low positive accommodation, and the mid-Judith discontinuity is a maximum regressive surface (MRS), marking a change to the mud-rich alluvial and paralic Coal Ridge Member, a shift to significantly higher rates of sediment accumulation, and marine transgression (T) by shoreface sands of the Woodhawk Member. New $^{40}Ar/^{39}Ar$ ages presented in this report are shown in italics. One legacy $^{40}Ar/^{39}Ar$ age of 77.52 ± 0.19 Ma (sanidine) from a bentonite ~265 m above the base of the Two Medicine Formation (Foreman et al. 2008) was recalculated to 78.02 ± 0.19 Ma. Rogers (1998) provisionally correlated the mid-Judith discontinuity with a widespread lacustrine carbonate interval (LCI) that overlies the aforementioned bentonite, ~330 m above the base of the Two Medicine Formation. Positions of Santonian-Campanian and Campanian-Maastrichtian boundaries (Ogg and Hinnov 2012) are approximated. SGA = Sweetgrass arch, across which Campanian/Maastrichtian strata have been eroded.

1973; Case 1978; Horner 1988; Fiorillo and Currie 1994; Prieto-Marquez 2005; Fricke et al. 2008, 2009; Tweet et al. 2008; Ryan et al. 2014).

Despite this long-standing significance, key aspects of the unit remain underdescribed and poorly understood. For example, most descriptions of the Judith River Formation in Montana characterize it as predominantly, if not wholly, terrestrial in origin, with only minor evidence of marine or brackish influence, whereas approximately half of the formation in the eastern half of the type area consists of shallow marine deposits (Stanton and Hatcher 1905; Rogers 1993, 1998; Rogers and Kidwell 2000). The existing composite type section of the formation, located in the western part of the type area (Sahni 1972), thus captures only part of the range of lithologies present in the formation. Moreover, although regional correlations are understood at a general level (fig. 2), precise correlations of the Judith River Formation with richly fossiliferous equivalents in western Montana (e.g., Two Medicine Formation) and Canada (e.g., Belly River Group) have remained elusive, in part because of a lack of published radioisotopic ages from the type area.

In this report, we re-examine the sedimentology of the Judith River Formation in its type area in the UMRBNM and propose three new reference sections that illustrate the full range of lithologies developed in the unit. One new reference section (92-JRT-15; figs. 1, 3) from the western edge of the type area spans the transition from the underlying Claggett Formation to the Judith River Formation. A second new reference section (91-JRT-8; figs. 1, 3), located in the middle of the type area, spans the entire formation from its basal contact with the Claggett Formation to its upper contact with the Bearpaw Formation. This complete section hosts a lithologic discontinuity, herein referred to as the mid-Judith discontinuity, that reflects a regional reorganization of terrestrial and marine depositional systems associated with a turnaround in correlative marine units from regressive to transgressive deposition (Rogers 1998). We present new data on mineralogical and facies shifts across this discontinuity—which is now recognized as extending northward into southern Alberta and Saskatchewan—and use it to subdivide the terrestrial part of the Judith River Formation into two new members. A third reference section (91-JRT-12; figs. 1, 3), located in the eastern portion of the type area, intersects the marine portion of the Judith River Formation, and a third formal member is erected to designate these distinctive marine-shoreface sandstones. New $^{40}Ar/^{39}Ar$ ages are reported for bentonite beds in two of the reference sections, and a third $^{40}Ar/^{39}Ar$ age is reported from a bentonite bed present ~5 m above the Judith River Formation–Bearpaw Formation contact. These new ages are the first from the type area of the Judith River Formation. On the basis of these new litho- and chronostratigraphic data, we subdivide the Judith River Formation into regionally traceable stratigraphic packages that accumulated under distinct accommodation regimes that are best explained by upstream tectonic controls (e.g., Catuneanu 2006; Eberth and Braman 2012).

## Methods

Forty-eight surface sections were measured in the outcrop belt of the Judith River Formation in north-central Montana. They provide a framework for sampling, a basis for stratigraphic analysis, and are integrated with raster image well logs (MJ Systems) to extend stratigraphic coverage to the plains of southern Canada. Well logs were ground truthed using nearby surface sections to confirm subsurface stratal signatures. Samples systematically collected from surface sections were used to assess compositional trends in framework and clay mineralogy. Standard 30-$\mu$m-thin sections were prepared and stained for the identification of K-feldspar. Four hundred grain counts were performed on a motorized Petrog Lite MicroStepper stage coupled to a Nikon Eclipse E600 petrographic microscope. All sand-sized grains in the fine to coarse size fraction were counted, with most falling in the fine to medium size range. Additional mineralogical information was gathered using scanning electron microscopy–energy-dispersive spectrometry, and backscatter electron images were collected to illustrate key compositional features. The clay fraction was recovered via centrifugation, and oriented mounts solvated with ethylene glycol were scanned on a PANalytical X'Pert PRO X-ray diffractometer with a Cu anode (45 kV, 40 mA) and goniometer radius of 240 mm. Sample scans were continuous and ranged from 3° to 40° 2$\theta$, spanning a 20-min scan interval. A semiquantitative approximation of clay mineral abundance in each sample was determined, using the reference intensity ratio method (Hillier 2003).

Bentonite samples for $^{40}Ar/^{39}Ar$ analysis were disaggregated with warm tap water and repeated agitation and sieved through 20-, 40-, 60-, and 100-mesh screens. Feldspar was separated from the residual coarse fraction with a Frantz isodynamic separator. Sanidine was isolated from plagioclase by density separations using heavy liquids. Sanidine concentrates (>300 $\mu$m fraction) were placed into wells in an aluminum disk before irradiation. The arrangement consisted of 12 wells (3.2 mm deep × 2.5 mm diameter) in an 18-mm-diameter circular configu-

ration, with the standards at the cardinal points and unknowns in remaining pits (Best et al. 1995). After additional protective packaging, the samples were irradiated for 90 h in the Cd-lined, in-core CLICIT facility of the Oregon State University TRIGA reactor. Sanidine from the Fish Canyon Tuff of Colorado was used as a mineral standard, with a reference age of 28.201 ± 0.046 Ma (Kuiper et al. 2008). The total $^{40}K$ decay constant used in the age calculations was $5.463 \pm 0.214 \times 10^{-10}$/yr (Min et al. 2000), and the atmospheric $^{40}Ar/^{36}Ar$ ratio was 298.56 ± 0.31 (Lee et al. 2006). Reactor-induced isotopic production ratios for this irradiation were as follows: $(^{36}Ar/^{37}Ar)_{Ca} = 2.65 \pm 0.02 \times 10^{-4}$, $(^{38}Ar/^{37}Ar)_{Ca} = 1.96 \pm 0.08 \times 10^{-5}$, $(^{39}Ar/^{37}Ar)_{Ca} = 6.95 \pm 0.09 \times 10^{-4}$, $(^{37}Ar/^{39}Ar)_{K} = 2.24 \pm 0.16 \times 10^{-4}$, $(^{38}Ar/^{39}Ar)_{K} = 1.220 \pm 0.003 \times 10^{-2}$, $(^{40}Ar/^{39}Ar)_{K} = 2.5 \pm 0.9 \times 10^{-4}$. The $^{40}Ar/^{39}Ar$ extractions were performed at the Berkeley Geochronology Center; a focused $CO_2$ laser was used to fuse and rapidly liberate trapped argon from individual sanidine crystals. Gasses were scrubbed with SAES getters for several minutes to remove impurities (CO, $CO_2$, $N_2$, $O_2$, and $H_2$), followed immediately by measurement of the purified noble gases for five argon isotopes on a MAP 215-50 mass spectrometer for ~30 min.

## Geologic Background

Original reference to the Judith River beds exposed along the Missouri River in north-central Montana is found in the study by Meek and Hayden (1856). Hayden (1871) subsequently proposed the term "Judith group" to refer to strata near the confluence of the Judith and Missouri rivers (fig. 1), and shortly thereafter Meek (1876) introduced the term "Judith River group" for strata at the mouth of the Judith River. Stanton and Hatcher (1903, 1905) defined the Judith River group to lie between the underlying Claggett Formation and overlying Bearpaw Formation. The term "Judith River formation" began to appear in the literature in the early 1900s (Lambe 1907; Knowlton 1911; Peale 1912; Stebinger 1914; Bowen 1915, 1920) and has been employed for a more than a century since to refer to strata between the Claggett and Bearpaw Formations in Montana and the Pakowki and Bearpaw Formations in Canada (e.g., Weimer 1960, 1963; Ostrom 1964; McLean 1971; Sahni 1972; Case 1978; Wood et al. 1988; Wood 1989; Brinkman 1990; Eberth 1990; Thomas et al. 1990). In the early 1990s, Eberth and Hamblin (1993) proposed that the formation be elevated to group rank in both Canada and Montana and that the revised Judith River Group include the Foremost, Oldman, and Dinosaur Park Formations. Extending this nomenclature across the international border was complicated by the traditional inclusion of the Judith River Formation within the Montana Group of Eldridge (1888, 1889). Moreover, the petroleum industry in western Canada declined to adopt the elevation in rank of the Judith River Formation, opting instead to maintain reference to the long-standing Belly River series, which was formalized to group status by Jerzykiewicz and Norris (1994). As a result, Hamblin and Abrahamson (1996) concluded that the term "Judith River Group" should be abandoned and that "Belly River Group" should be used throughout the plains of southern Alberta and Saskatchewan to refer to strata bound by the Pakowki and Bearpaw Formations.

Rocks of the Judith River Formation constitute the distal part of an eastward-thinning clastic tongue of terrestrial and shallow marine strata (fig. 2) that accumulated during regression of the Claggett Sea and subsequent transgression of the Bearpaw Sea (R8 and T9 of Kauffman 1977). Within Montana, the Judith River Formation correlates to the west with terrestrial deposits of the middle and upper Two Medicine Formation (Lorenz 1981; Rogers 1995, 1998) and is intercalated between open marine deposits of the Claggett and Bearpaw Formations (Stanton and Hatcher 1905; Gill and Cobban 1973; fig. 2). To the east, where the Judith River clastic tongue pinches out, the Claggett and Bearpaw Formations coalesce to form the Pierre Formation. To the north, in the plains of Alberta and Saskatchewan, the Judith River Formation correlates with the Foremost, Oldman, and Dinosaur Park Formations of the Belly River Group (Eberth and Hamblin 1993; Jerzykiewicz and Norris 1994; Hamblin and Abrahamson 1996; Eberth 2005). To the south, the Judith River Formation is recognized as part of the Mesaverde Group in the Big Horn Basin of Wyoming and correlates, at least in part, with the Wahweap and Kaiparowits Formations in southern Utah, the Fruitland Formation in New Mexico, and the Aguja Formation in West Texas (Weimer 1960, 1963; Lawton 1986; Klug 1993; Roberts et al. 2005, 2013; Jinnah et al. 2009).

Radioisotopic ages from the Judith River Formation in northern Montana (Goodwin and Deino 1989) and correlative Two Medicine Formation in northwestern Montana (Rogers et al. 1993; Foreman et al. 2008) indicate that the Judith River Formation in the plains of central Montana accumulated during the mid- to late Campanian (Ogg and Hinnov 2012; Cohen et al. 2013). Radioisotopic dating of bentonite beds within the Belly River Group in Alberta also yields Campanian ages (Eberth et al. 1992; Eberth 2005). Biostratigraphic data derived from

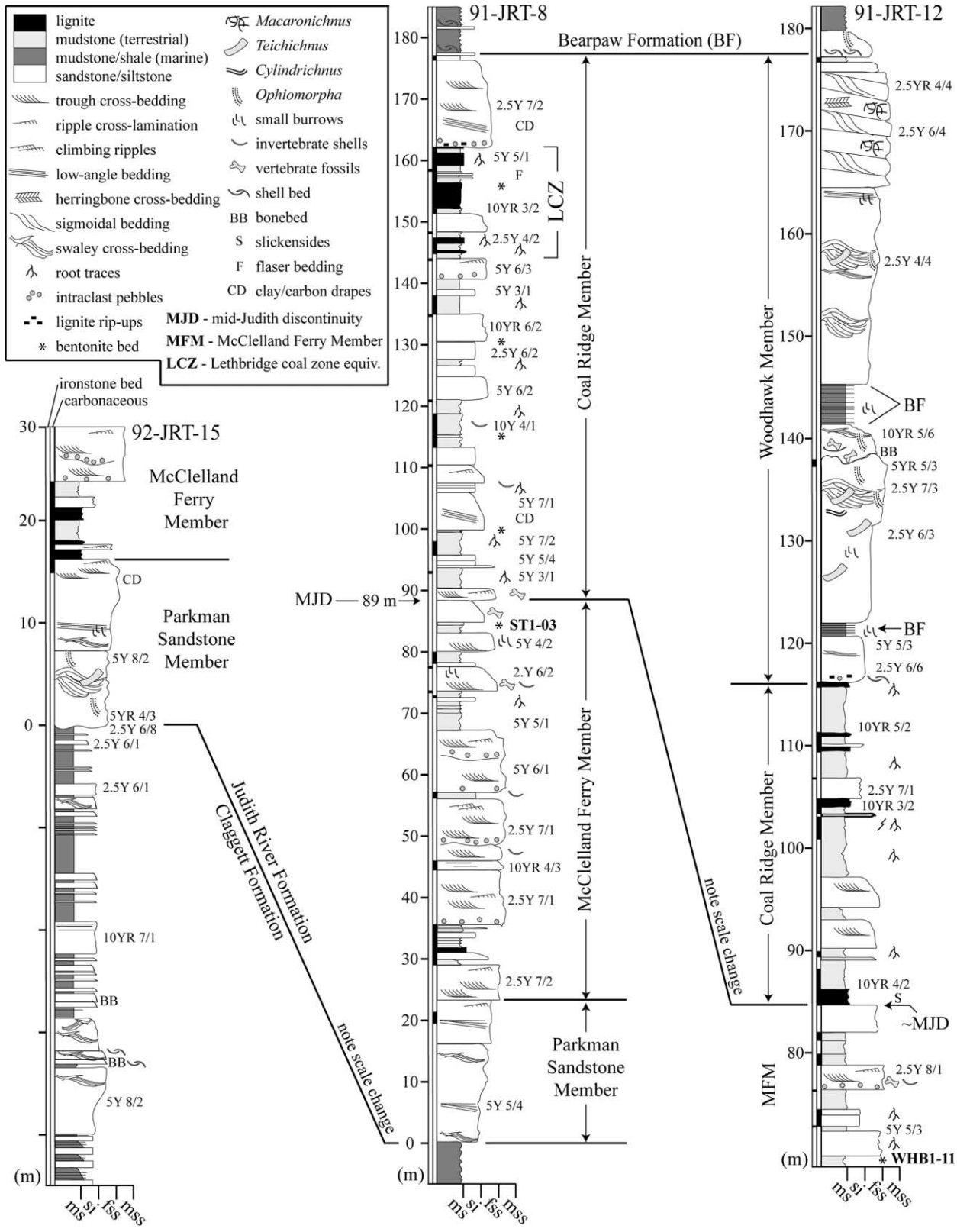


**Figure 3.** Three newly proposed reference sections of the Judith River Formation. Section 92-JRT-15 on the Judith River near Dog Creek spans the basal 30 m of the Judith River Formation and several tens of meters of the underlying Claggett Formation and clarifies the disconformable nature of the lower contact. Section 91-JRT-8 on the left bank of the mainstem Missouri River spans the entire Judith River Formation from the basal contact with the Claggett Formation to the upper contact with the Bearpaw Formation. This section affords a complete bottom-to-top per-

marine invertebrates (Gill and Cobban 1973) and palynomorphs (Tschudy 1973) are consistent with a Campanian age.

## New Lithologic Observations and Reference Sections

In the first comprehensive treatment of the Judith River Formation, Stanton and Hatcher (1905) delimited the type area, defined and described lower and upper contacts, and published descriptions of stratigraphic sections measured on Birch Creek, Dog Creek, and Cow Creek (fig. 1). One of the notable observations of Stanton and Hatcher (1905, p. 42) was the apparent inclusion of a "strictly marine horizon" within the upper half of the Formation. This interpretation was based on paleontologic evidence, specifically the occurrence of mosasaur bones, shark teeth, and marine invertebrates in a section measured along the east side of Cow Creek (fig. 1).

The type section of the Judith River Formation was established by Sahni (1972) as part of a study devoted to the formation's vertebrate fauna. He could not locate a complete section of the formation in the western part of the type area where the formation is thickest and thus proposed a composite stratotype in the vicinity of Birch Creek (fig. 1). Both lower and upper contacts were interpreted as gradational, and the total thickness was estimated to be 168 m. Sahni (1972) published graphic logs of his composite type section but scant lithologic detail. He interpreted the formation to be predominantly terrestrial or brackish and noted that vertebrate fossils were particularly abundant in the upper half of the unit.

The new reference sections described here (fig. 3) supplement the original composite type section of Sahni (1972) in three important ways. First, they include more detailed information relating to lithology, fossil content, and formation contacts relevant to paleoenvironmental and sequence stratigraphic interpretation. Second, one of the new reference sections (91-JRT-8) spans the entire Judith River section and thus provides a complete bottom-to-top record of the unit's lithology and depositional history. Last, together the three reference sections illustrate previously unrecognized lithologic heterogeneity developed both in vertical section and parallel to depositional dip, and they exemplify the full spectrum of lithologies that characterize the Judith River Formation in the type area. They provide the documentary basis for the formal lithostratigraphic subdivision of the formation into new subunits at member rank. The three new members of the Judith River Formation proposed below are worthy of formal lithostratigraphic recognition because they are (1) distinctive in lithology from surrounding beds; (2) readily identified in outcrop, on aerial photographs, and in satellite imagery; and (3) significant to geological history, particularly in relation to evidence for regional base level change in both terrestrial and marine depositional systems during the Bearpaw transgression. They are also (4) mappable over >100 $km^2$ (at a 1:24,000 scale), although member rank units need not meet this criterion (NACSN 2005).

***New Reference Section 92-JRT-15, Basal Contact of Judith River Formation.*** This section is located on the western edge of the type area on the right bank of a large east-west trending coulee that intersects the Judith River floodplain approximately 5 km upstream from the confluence of the Judith and Missouri Rivers (47°41′29.8″N, 109°37′25.2″W; NE 1/4 SE 1/4 S11, T22N, R16E; fig. 1). It is readily accessible from PN Bridge Road (Montana Highway 236) that connects the town of Winifred to Judith Landing. The section spans the basal 30 m of the Judith River Formation and several tens of meters of the underlying Claggett Formation (figs. 3, 4*A*).

Interbedded gray shales, tan siltstones, and subsidiary pale yellow fine-grained sandstones of the marine Claggett Formation compose the lower 43 m of the section (figs. 3, 4*A*). Shale beds are microlaminated and include thin (millimeter-scale) wavy laminae and lenses of siltstone and dispersed centimeter-scale carbonate concretions. Bedding planes are occasionally draped with millimeter-scale fragments of carbonaceous plant debris. Interbedded siltstones to fine sandstones are thinly bedded, exhibit both planar lamination and swaley cross lamination, and—especially in the lower part of the

spective on lithology, contacts, and depositional history and serves as the stratotype for the new McClelland Ferry (MFM) and Coal Ridge (CRM) Members of the Judith River Formation. MJD = mid-Judith discontinuity, LCZ = Lethbridge coal zone equivalent. Section 91-JRT-12 on the right bank of the mainstem Missouri River just below Cow Creek spans the upper 110 m of the Formation and serves as the stratotype for the new Woodhawk Member of the Judith River Formation. Bentonite beds ST1-03 (76.24 ± 0.18 Ma) and WHB1-11 (76.17 ± 0.07 Ma) are indicated in sections 91-JRT-8 and 91-JRT-12, respectively. Note that the vertical scale varies among sections.

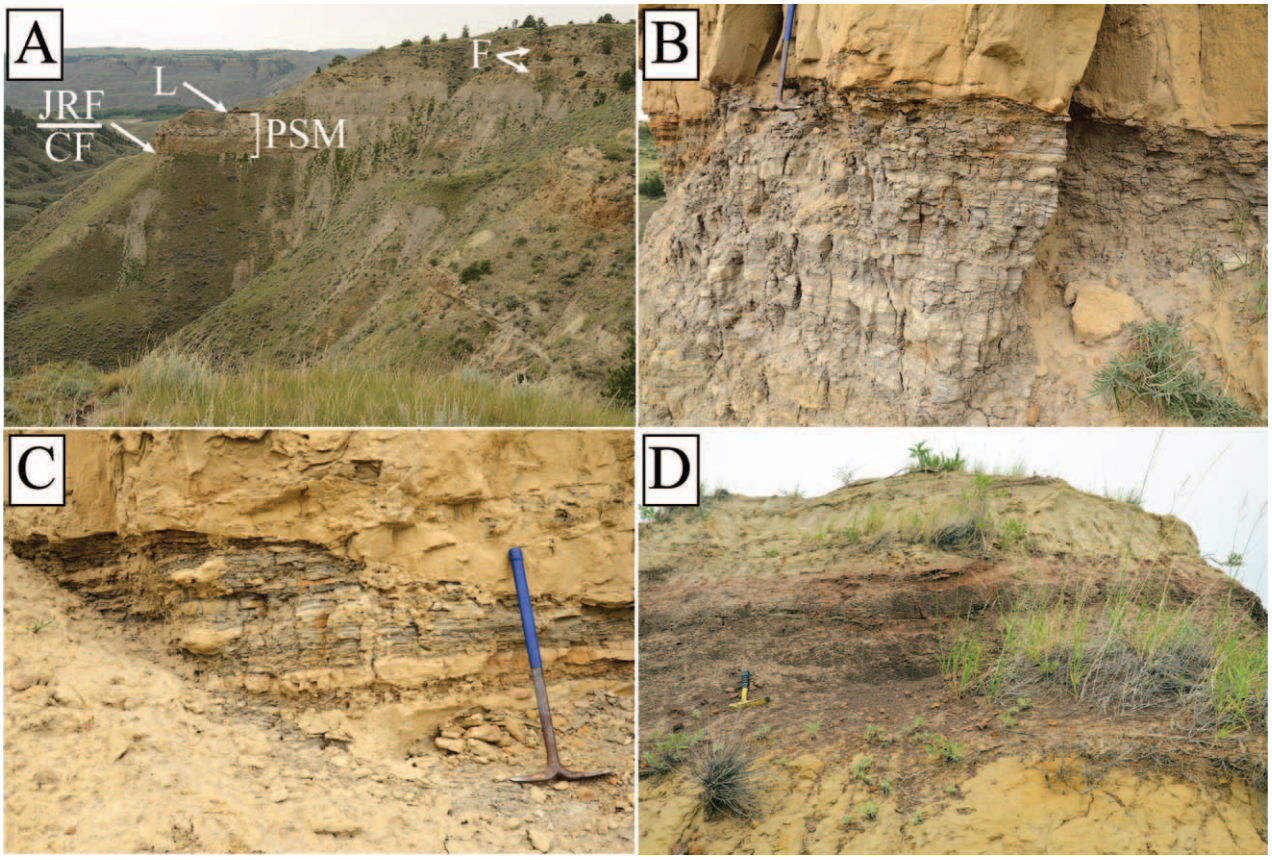


**Figure 4.** Outcrop views of 92-JRT-15 reference section. *A*, View of section locality, showing sharp contact of the Parkman Sandstone Member (PSM) of the Judith River Formation (JRF) on shales of the Claggett Formation (CF), base of the lignite-rich zone (L) within the JRF, and fluvial sandstone bodies (F) low in JRF section. *B*, Sharp contact separating Parkman Sandstone Member from shales of Claggett Formation. *C*, Erosional relief of up to 2 m is developed at contact. *D*, A lignite-rich interval of paralic facies caps the Parkman Sandstone Member throughout the Judith River Formation type area.

section—host localized concentrations of vertebrate and invertebrate bioclastic debris, including bone sand.

The boundary between the Claggett Formation and the overlying Judith River Formation, as positioned by previous workers and here, is a sharp contact with 2 m of erosional relief over lateral scales of ~5 m (fig. 4*B*, 4*C*). This disconformity is overlain by a widespread, ~16-m-thick, massively parted cliff of tan and light gray, fine- to medium-grained sandstone (fig. 4*A*). It exhibits swaley cross-bedding, small-scale low-angle trough cross-bedding, planar lamination, and limonite-stained burrow casts of *Teichichnus*, *Ophiomorpha*, and, at its top, *Skolithos*. Ironstone concretions and thin carbonaceous drapes are developed in the upper few meters of this basal sandstone sheet, which has been interpreted to represent prograding shoreface and foreshore deposits (Rogers 1993, 1998). Previous reports have referred to this basal sandstone as the *Tancredia* Sandstone (Lindvall 1962; Sahni 1972) and the Parkman Sandstone Member (e.g., Knechtel and Patterson 1956; Gill and Cobban 1973; Fiorillo 1991; Rogers 1998). We follow existing practice and refer to the extensive basal sandstone unit of the Judith River Formation as the Parkman Sandstone Member. Although previous reports (e.g., Sahni 1972; Fiorillo 1991) have characterized the contact between the Parkman Sandstone Member and underlying Claggett Formation as gradational and conformable, our work indicates that the boundary is erosional at a regional scale, consistent with the onset of forced regression.

Lignite beds, carbonaceous mudstones, and muddy, fine-grained sandstones overlie the Parkman Sandstone Member and indicate a shift to coastal terrestrial sedimentation (fig. 4*D*). The 7.5-m-thick, lignite-rich interval of paralic facies is sharply overlain by an ~6-m-thick, fine- to medium-grained fluvial sandstone body characterized by 20–50-cm sets of tabular

and high-angle trough cross-bedding and intraclast lag deposits. This sandstone body signals an abrupt shift from coastal mire facies to fluvial deposition consistent with more inland settings and lies at the top of the local section (figs. 3, 4*A*).

***New Reference Section 91-JRT-8, Complete Section of Judith River Formation.*** This section is located on the left bank of the Missouri River at the southern tip of Coal Ridge (47°45′34.7″N, 109°19′56.8″W; SW 1/4 SE 1/4 S18, T23N, R19E; fig. 1), approximately 23 km northeast of section 92-JRT-15. It is readily accessible from Lloyd Road, which connects Stafford/McClelland Ferry to ranches and communities to the north of the Missouri River. At this locality, the entire Judith River Formation section is exposed, with a total thickness of 177 m (figs. 3, 5*A*).

Shales and siltstones of the underlying Claggett Formation are poorly exposed but can be exhumed via trenching. Exposure of the Parkman Sandstone Member of the Judith River Formation is also rather limited, but its outcrop belt is effectively delimited by ledges of fine sandstone with swaley bedding and by ponderosa pine trees that have gained a foothold in weathered slopes of these sandy strata (fig. 5*A*). As in section 92-JRT-15, the contact between the Parkman Sandstone Member of the Judith River Formation and the underlying Claggett Formation is sharp and presumably disconformable, although limited outcrop prohibits the identification of erosional relief (fig. 5*B*). The Parkman Sandstone Member is overlain by a 13-m-thick zone of lignite and carbonaceous mudstone (fig. 3) interbedded with fine-grained sandstone bodies characterized by recessive weathering and clay and carbon drapes, signaling coastal mire sedimentation. These paralic beds are capped sharply by ~55 m of more resistant fine- to medium-grained sandstone bodies with medium- to large-scale, high-angle trough and tabular cross-bedding (fig. 5*A*, 5*C*). These resistant sandstone sheets of fluvial origin, some of which are multistory, render the lower portion of the Judith River section decidedly blocky and stairstep-like in appearance and support only sparse modern vegetation.

Finer-grained facies, including thinner and finer-grained fluvial sandstone bodies, predominate in the upper ~90 m of the Judith River section within the 91-JRT-8 reference section (fig. 5*A*, 5*C*, 5*D*). These fine-grained facies produce steeper, smoother slopes and are more sparsely vegetated. Concomitant with the shift to finer-grained strata is an increase in the abundance of carbonaceous deposits, including lignite beds, organic-rich mudstones (fig. 5*E*), and carbon drapes in cross-bedded sandstone facies; the latter includes well-developed inclined heterolithic stratification in nearby exposures (fig. 5*F*). Several discrete bentonite beds are also preserved in this upper 90 m of 91-JRT-8 (fig. 3). The abrupt change in the nature of the Judith River alluvial record evident in 91-JRT-8 was identified by Rogers (1993, 1998) throughout the type area and interpreted as a widespread lithologic discontinuity linked to a subsidence-driven reorganization of alluvial depositional systems. New insights into compositional changes across this discontinuity and new data that pertain to its diagenesis and regional extent are presented in detail below.

The upper contact of the Judith River Formation with the Bearpaw Formation in reference section 91-JRT-8 is marked by a deposit of disarticulated oyster shells that ranges from a single valve pavement to a 20-cm-thick bed of packed shell debris. This shell bed, which can be traced widely throughout the type area, separates massive carbonaceous mudstone of the Judith River Formation from marine siltstones and silty to fissile shales of the overlying Bearpaw Formation (fig. 3).

***New Reference Section 91-JRT-12, Upper Marine Unit of Judith River Formation.*** This section is located at the mouth of Woodhawk Creek in the eastern portion of the Judith River Formation type area (47°44′48.9″N, 108°57′2.9″W; NE1/4 NW1/4 S19, T23N, R22E; figs. 1, 6*A*), approximately 28 km to the east of section 91-JRT-8. At this locality, exposures span the upper ~110 m of the Judith River Formation and the contact with the overlying Bearpaw Formation (fig. 3). The lithology of the Judith River Formation here is markedly distinct from western reaches of the type area (compare with 91-JRT-8). Access is afforded by Woodhawk Bottom Road.

The lowest 48 m of reference section 91-JRT-12 consist of interbedded mudstones (dominant), lignites, and thin- to thick-bedded siltstones and sandstones (fig. 6*B*, 6*C*). Beds of mudstone preserve small root traces and abundant carbonaceous debris and are interstratified with numerous beds of brown to black fissile lignite. Siltstone interbeds are typically massive and also yield abundant plant debris. Fine- to medium-grained gray sandstone bodies at the base of section 91-JRT-12 are characterized by medium-scale trough and tabular cross-bedding with local carbon drapes. This terrestrial succession is overlain by a distinctly more cliff-forming, 62-m-thick interval dominated by massively parted, tan to yellow, fine- to medium-grained sandstones of shallow marine and deltaic origin, described in more detail below (Rogers 1995, 1998; Rogers and Kidwell 2000). The contact between the terrestrial and overlying marine facies is sharp and mantled by a thin, patchy veneer of

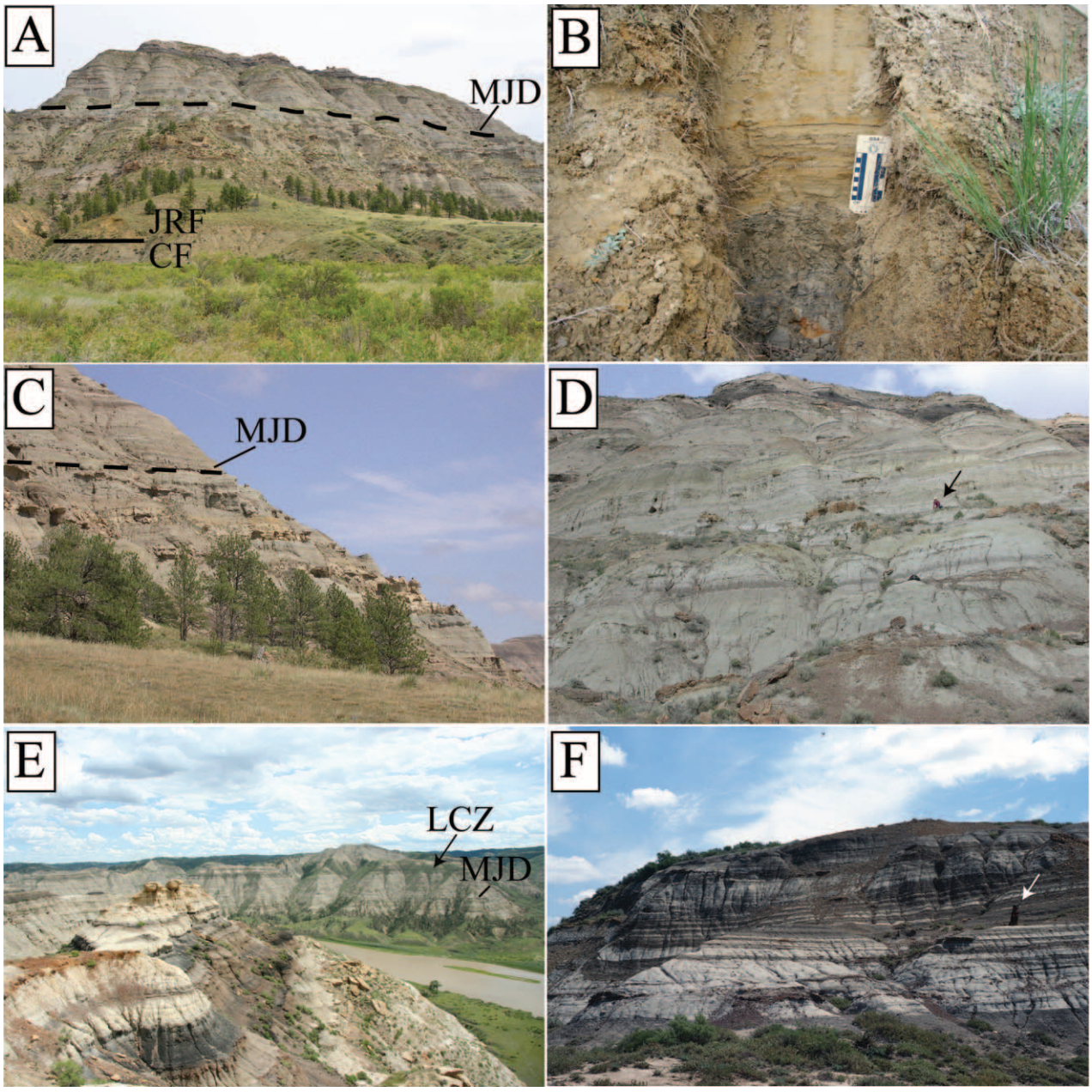


**Figure 5.** Outcrop views of 91-JRT-8 reference section. *A*, View of entire section, showing basal contact between Judith River Formation (JRF) and Claggett Formation (CF) and position of mid-Judith discontinuity (MJD; dashed line). *B*, Close-up view of sharp basal contact of the Parkman Sandstone Member of Judith River Formation on the underlying Claggett Formation. *C*, Sandstone-dominated exposures of lower Judith River Formation below the mid-Judith discontinuity (MJD). Ponderosa pines in this view and in *A* are rooted in the Parkman Sandstone Member. *D*, Mudstone-dominated exposures of the upper Judith River Formation above the mid-Judith discontinuity. Arrow points to person for scale. *E*, Carbonaceous facies characteristic of upper Judith River Formation. A distinctive lignite-rich interval within the upper ~20 m of the formation correlates lithologically with the Lethbridge Coal Zone known from core and outcrop in the Dinosaur Park Formation in Canada. Arrow marks position of this prominent lignite zone on distant south (*right*) bank of Missouri River. Position of MJD indicated. *F*, Inclined heterolithic stratification developed near top of the Judith River Formation in exposures near reference section 91-JRT-8. Arrow points to 85-cm-tall dog for scale.

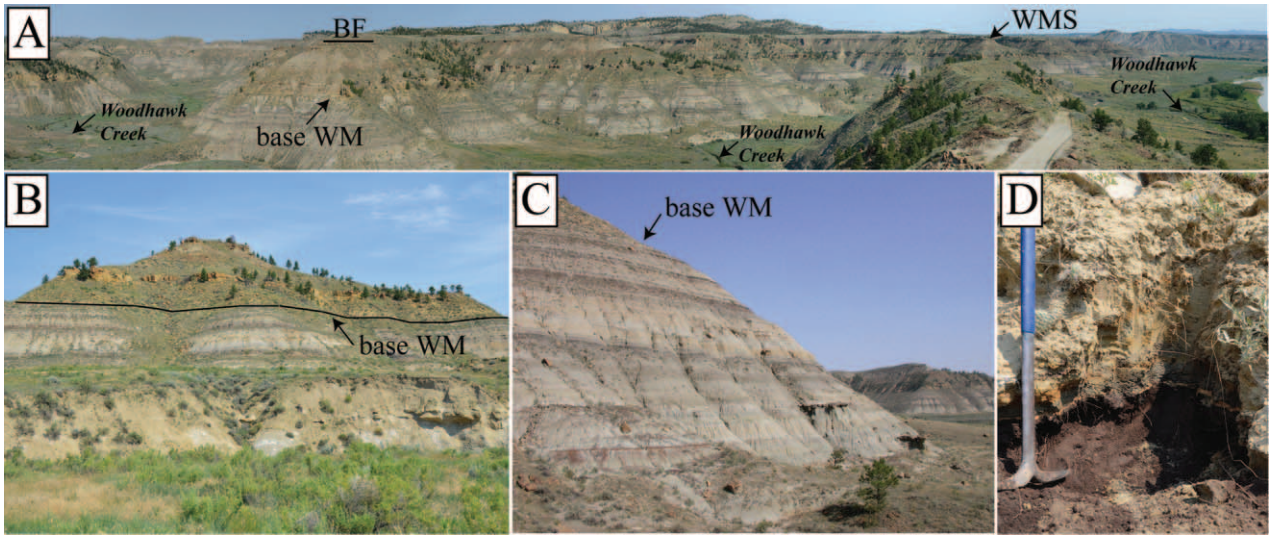


**Figure 6.** Outcrop views of the new Woodhawk Member. *A*, Panorama upstream (*left*) to downstream (*right*) of Woodhawk Creek drainage (Missouri River on far right edge) looking north from Woodhawk Bottom Road (47°44′ 24.9″N, 108°57′19.7″W), showing lateral expanse of shallow marine sandstones that form the Woodhawk Member (WM), its basal contact midway through the badland exposures of the Judith River Formation, and its upper contact with the overlying Bearpaw Formation (BF). WMS denotes the top of the stratotype section of the Woodhawk Member, which is on the left bank of Woodhawk Creek closest to its junction with the Missouri River. *B*, Outcrop along Woodhawk Creek in vicinity of stratotype, with contact marked between Woodhawk Member and underlying paralic facies. *C*, Interbedded mudstones, siltstones, sandstones, and lignites of terrestrial origin below the Woodhawk Member along Woodhawk Creek. *D*, Contact of Woodhawk Member on underlying bed of carbonaceous mudstone. A thin, patchy layer of mudstone rip-ups, bivalve shell debris, and fossil bone fragments mantles this contact.

lignite rip-ups, claystone intraclasts, bivalve shell debris, and fossil bone fragments (fig. 6*D*).

The marine sandstone-dominated interval forming the upper part of 91-JRT-12 can be traced throughout the eastern portion of the Judith River Formation type area, from outcrops in the vicinity of Sturgeon Island to Fred Robinson Bridge (fig. 7*A*). Upstream from Grand Island, the sandstone lithosome caps ridges along the mainstem Missouri River valley and major tributaries; it weathers orange-tan and is marked by stands of ponderosa pine (fig. 6). Downstream of Grand Island, this sandstone lithosome crops out at or near river level, where it creates steep exposures of gray sandstone capped by the Bearpaw Formation (fig. 7*B*).

In reference section 91-JRT-12, this sandstone lithosome consists in detail of a series of massive fine- to medium-grained sandstone bodies with thinner intervals of recessive laminated fines and skeletal or other fragmental lags. The basal 5 m of the sandstone lithosome consists of deeply weathered muddy sandstone with faint low-angle trough to swaley cross-laminations and a basal lag of mudstone rip-ups and mollusk shells. This basal sandstone is capped by a 1.3-m-thick recessive interval of interbedded shale and laminated siltstone that represents a thin tongue of the Bearpaw Formation (figs. 3, 8*A*). The next major sandstone ledge is characterized by swaley cross-bedding and a trace fossil assemblage that includes *Teichichnus*, *Ophiomorpha*, *Cylindrichnus*, and *Skolithos* (fig. 8*B*–8*D*). These predominantly fine-grained sandstones, interpreted as wave-influenced shoreface deposits, coarsen upward over a span of ~15 m to a cemented ledge that can be traced throughout Woodhawk Creek drainage and into surrounding areas (fig. 8*E*). This distinctive orange ledge is cemented by ferroan dolomite (fig. 8*F*, 8*G*) and capped by localized scours with concentrations of shark teeth, fish and marine reptile bones, shell debris, siderite pebbles, and reworked cemented burrow fills (fig. 8*H*). The succession of shallow marine facies overlying this ledge is similar to the underlying sequence, although the interbedded shale/siltstone package (Bearpaw Formation) is thicker (~4 m), and the shoreface sandstones coarsen up-section to a package of medium-grained sandstone characterized by bidirectional cross-bedding (fig. 9*A*, 9*B*); sigmoidal cross-bedding (fig. 9*C*); localized zones intensely bioturbated by *Macaronichnus* (fig. 9*D*); and, in its uppermost part, carbon drapes, silicifed wood,

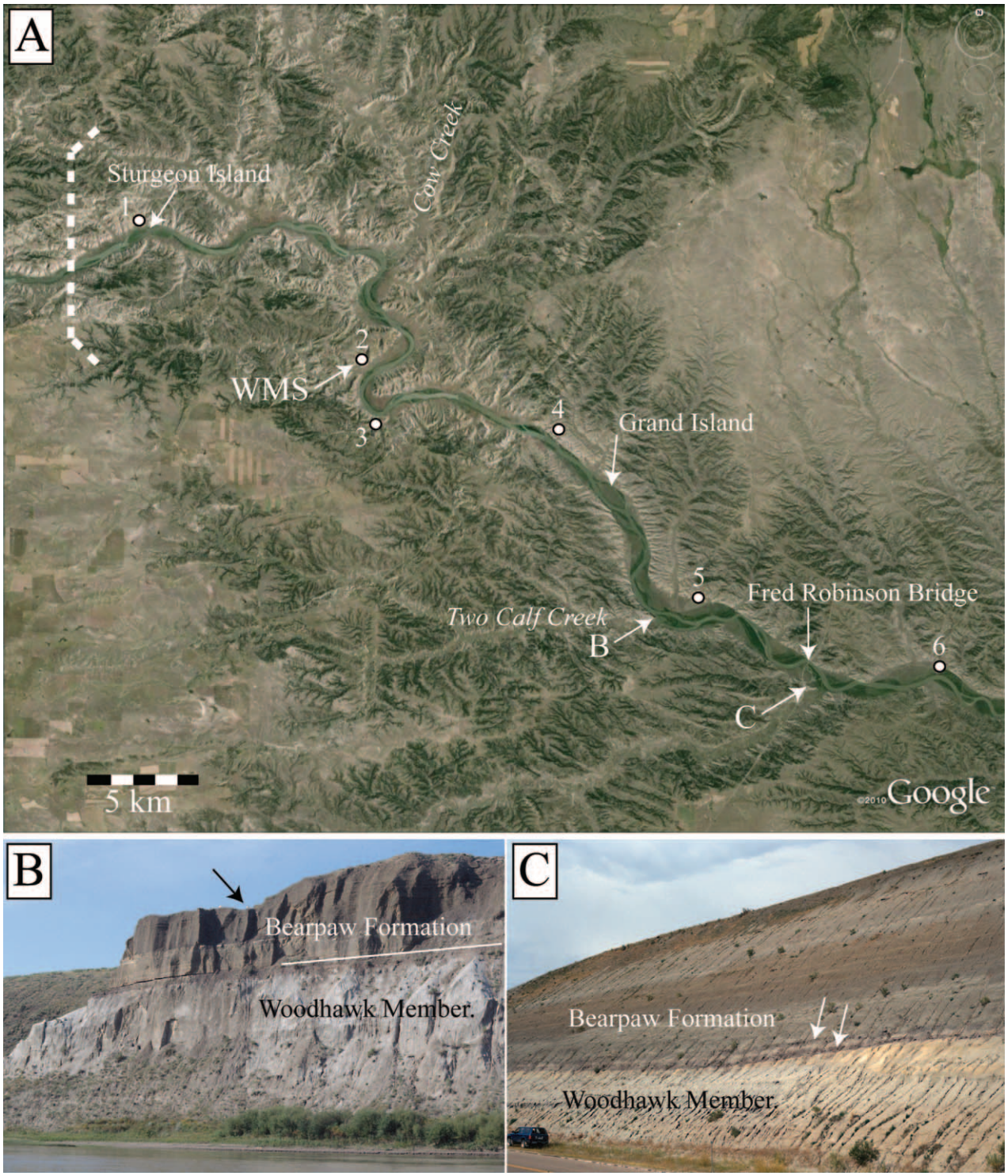


**Figure 7.** Outcrop belt of Woodhawk Member. *A*, Satellite image of eastern portion of Judith River Formation type area in Upper Missouri River Breaks National Monument. The Woodhawk Member can be traced on outcrop throughout this eastern portion of the type area, from the vicinity of Sturgeon Island to a few kilometers downstream of Fred Robinson Bridge. Numbered localities refer to sections in figure 10. WMS = Woodhawk Member stratotype. Modified from Google Earth. *B*, Downstream from Grand Island, the basal sequence (above D1; see fig. 10) of the Woodhawk Member crops out at river level, where it assumes steep exposures of gray sandstone. White line marks the contact with superjacent silty shales of the Bearpaw Formation. Arrow points to mountain sheep for scale. *C*, Top of the same basal sequence (above D1) of the Woodhawk Member along Montana Highway 191 immediately south of Fred Robinson Bridge, with two beds of carbonaceous mudstone (arrows) visible immediately below the contact with Bearpaw Formation.

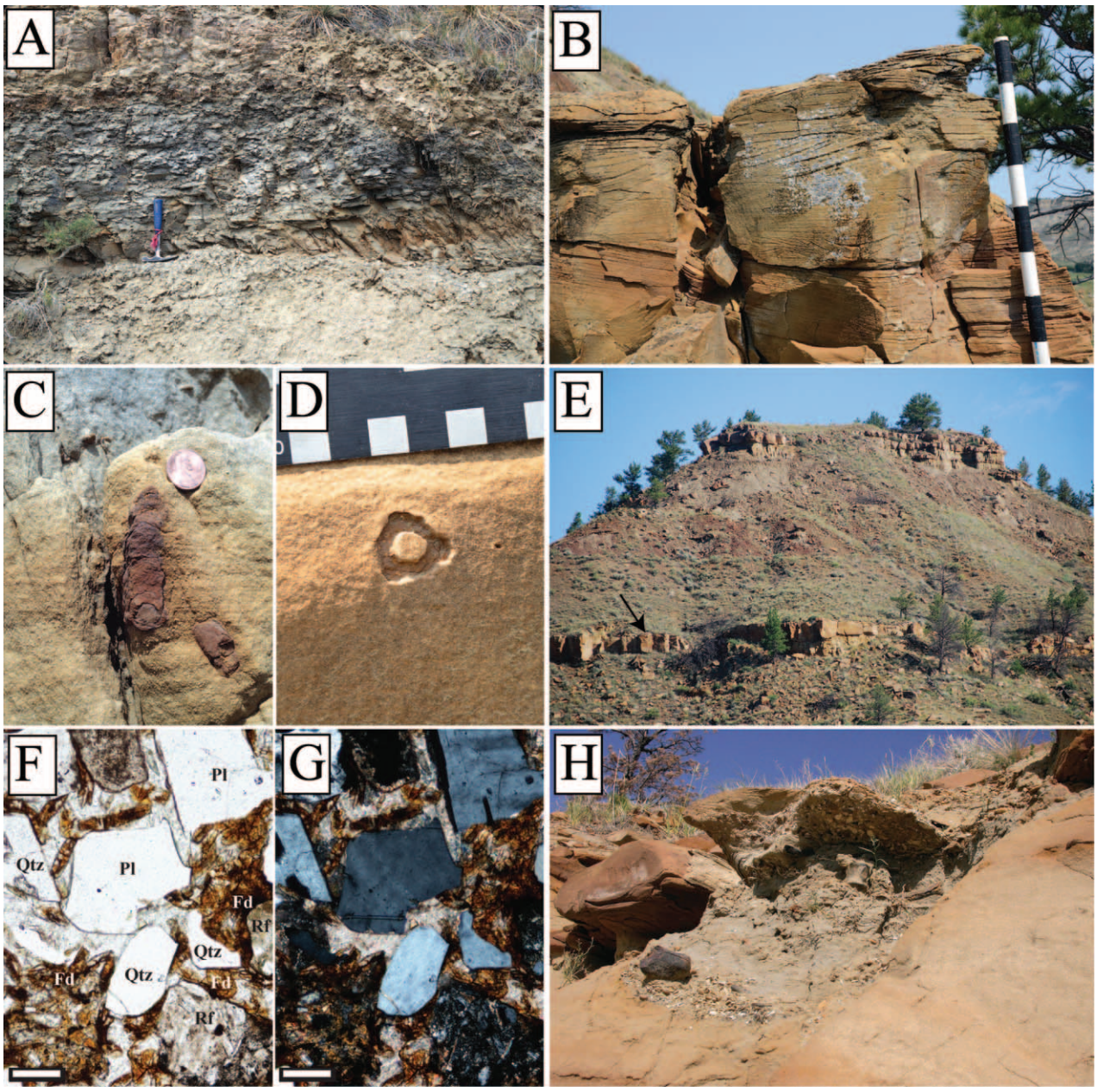


**Figure 8.** Sedimentary features of the Woodhawk Member. *A*, An interval of interbedded shale and laminated siltstone, representing maximum flooding, crops out a few meters above the base of each of the three high-frequency depositional sequences within the Woodhawk Member. *B*, Swaley cross-bedded sandstone is characteristic of the Woodhawk Member. *C*, *Teichichnus* is relatively common in exposures of the Woodhawk Member. *D*, *Ophiomorpha* is present in exposures of the Woodhawk Member and particularly abundant in the upper meter of the unit. *E*, A distinctive orange-weathering ledge (arrow) cemented by ferroan dolomite can be traced throughout Woodhawk Creek drainage and into surrounding areas. The top of this ledge marks the contact between the middle (above D2) and upper (above D3) depositional sequences of the Woodhawk Member. *F*, *G*, Plane- and polarized-light photomicrographs of ferroan dolomite cement from ledge in E (scale bars = 200 $\mu$m; Qtz = quartz, Pl = plagioclase, Rf = rock fragment, Fd = ferroan dolomite). *H*, The distinctive orange ledge is capped by localized scours marked by concentrations of shark teeth, fish and marine reptile bones, shell debris, siderite pebbles, and reworked cemented burrow casts.

and oyster shell pavements (fig. 9*E*). The meter-scale beds within this upper sandstone facies (fig. 9*A*) constitute a 12-m-thick set of southeastward-dipping clinoforms (fig. 9*F*, 9*G*) and are interpreted to represent tidally influenced delta front deposits that prograded into shallow marine environments of the Bearpaw Sea. A thin bed of carbonaceous mudstone and a poorly exposed bed of massive sandstone culminate the Judith River Formation in this reference section. The carbonaceous mudstone bed is overlain by a pavement of disarticulated oyster valves (fig. 9*E*), which in turn is overlain by the marine-shelf clay-rich siltstones and silty shales of the superjacent Bearpaw Formation.

## Formal Changes to Judith River Lithostratigraphy

***Woodhawk Member of the Judith River Formation.*** Reference section 91-JRT-12 is herein proposed as the stratotype of the new Woodhawk Member of the Judith River Formation (fig. 3). Formally naming this unit will facilitate reference to the relatively thick and widespread tongues of distinctive shallow marine sandstones that exist between the fluvial channel and overbank deposits of the Judith River Formation and the offshore (below fair-weather wave base) marine shales of the Bearpaw Formation in the eastern portion of the Judith River type area. A schematic cross section illustrating the dip-parallel expression of the Woodhawk Member is provided in figure 10. In outcrops and well logs, sandstones of the member can be tracked ~35 km parallel to depositional dip along the Missouri River corridor and for approximately 35 km parallel to depositional strike (north-south) in tributary drainages, including Cow Creek, Woodhawk Creek, Suction Creek, and Two Calf Creek (fig. 7).

Strata constituting the Woodhawk Member in the Judith River type area have been interpreted previously as three shallow-marine high-frequency sequences linked to the onset of the Bearpaw transgression in central Montana (Rogers 1993, 1998; Rogers and Kidwell 2000; fig. 2). Each sequence is ~30 m thick and includes a basal transgressive component of fine-grained sandstone spanning a few meters, with maximum water depth (labeled maximum flooding interval [MFI] in fig. 10) corresponding to an interval of interbedded shale and laminated siltstone (figs. 3, 8*A*). Above each MFI, wave-influenced shoreface strata generally coarsen and shallow upward to deltaic and paralic facies, including carbonaceous deposits of coastal mires and tidally influenced fluvial facies. Disconformities with evidence of conspicuous deepening (D1–D4, fig. 10) bound each of the three sequences, and these surfaces have been interpreted as composite in nature, representing transgressive surfaces coalesced onto sequence boundaries (Rogers and Kidwell 2000). Each deepening phase was considered to be sufficiently appreciable to categorize the cyclic units as high-frequency sequences (sensu Mitchum and Van-Wagoner 1991) rather than as parasequences. Each successively younger sequence backsteps progressively more landward (westward) in this retrogradational composite sequence set. The two upper sequences (above D2 and D3) are represented in full in the stratotype section at the mouth of Woodhawk Creek (figs. 3, 6, 8–10) and form the distinctive orange-tan sandstone outcrops that stretch from Bullwhacker Creek (47°48′31.9″N, 108°59′41.9″W) to the vicinity of Grand Island (47°41′53.5″N, 108°48′5.9″W). The D3 sequence boundary separating these two sequences is positioned at the top of the conspicuous orange ledge (fig. 8*E*) that can be tracked throughout Woodhawk Creek drainage and beyond. It is a sand-on-sand erosional contact marked by a shift to finer-grained sandstone above the boundary, distinctive diagenesis in the form of ferroan dolomite cement beneath the boundary (sensu McKay et al. 1995; Taylor et al. 1995; Taylor and Gawthorpe 2003; Taylor and Machent 2010), and associated localized lags of bioclastic debris, including shark teeth and marine reptile bones (fig. 8*F*–8*H*). These strata almost certainly yielded the marine fossils that prompted Stanton and Hatcher (1905, p. 42) to conclude that "strictly marine" facies were present in the upper 30 m of the Judith River Formation on nearby Cow Creek (fig. 7). Downstream of Grand Island (fig. 7), sandstones of the Woodhawk Member pinch out within marine shales of the Bearpaw Formation. The basal (above D1) depositional sequence of the Woodhawk Member can be observed in outcrop in the vicinity of Grand Island and can be traced downstream for several kilometers below Robinson Bridge, where it crops out at river level and eventually dives to the subsurface (figs. 7, 10).

***McClelland Ferry and Coal Ridge Members of the Judith River Formation.*** Reference section 91-JRT-8 is proposed as the stratotype for two new members in the terrestrial portion of the Judith River Formation: the McClelland Ferry Member and superjacent Coal Ridge Member (figs. 3, 11). Formally naming these two units enhances understanding of currently undifferentiated terrestrial strata that represent most of the formation and promotes a more regional perspective on nonmarine sedimentation patterns. The sandstone-dominated McClelland Ferry Member can be traced from the western limits of the type area, where it is exposed in its entirety, to Woodhawk Bottom, where only the upper few me-

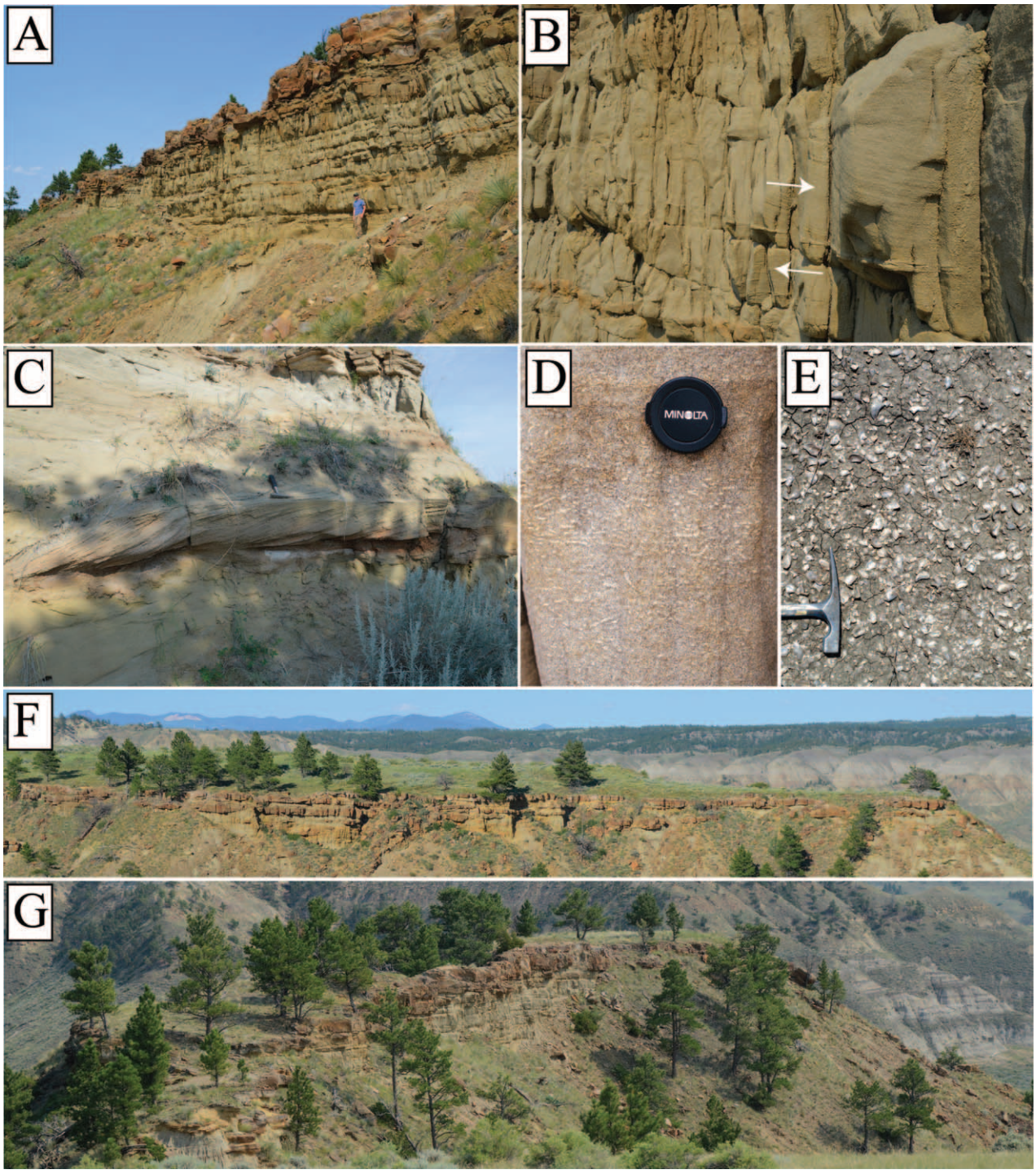


**Figure 9.** Top of Woodhawk Member. *A*, Woodhawk Member is capped by an ~12-m-thick interval of thick (meter-scale) bedded medium-grained sandstone with tidal indicators. *B*, Bidirectional cross-bed sets. *C*, Sigmoidal bedding. *D*, The trace fossil *Macaronichnus* is locally abundant. *E*, A thin, patchy, oyster-shell pavement locally caps the Woodhawk Member along Woodhawk Creek. *F*, *G*, Views of southeastward-dipping (to the right in these photos) clinoforms capping the Woodhawk Member. These beds are interpreted to represent tide-influenced delta front deposits that prograded into the Bearpaw Sea. View in *F* caps a ridge immediately to the northeast of the Woodhawk Member stratotype. View in *G* caps the ridge that includes the Woodhawk Member stratotype section.

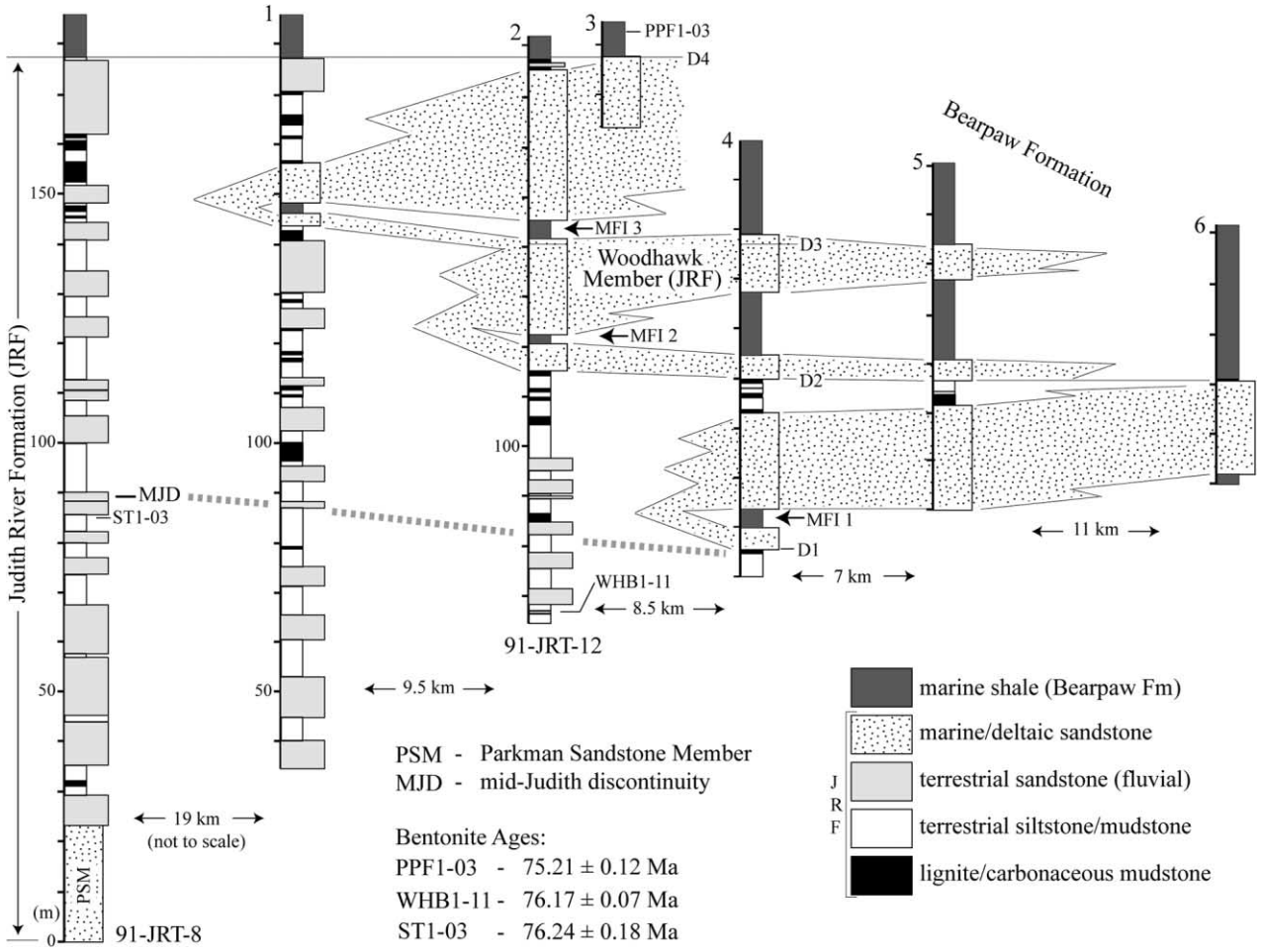


**Figure 10.** Dip-parallel cross section illustrating the three high-frequency depositional sequences that constitute the Woodhawk Member (stippled) in the Judith River Formation type area. Each sequence includes a basal transgressive package of fine-grained marine sandstone spanning a few meters, with maximum water depth (maximum flooding interval [MFI] 1–3) corresponding to packages of interbedded shale and laminated siltstone of the Bearpaw Formation (see figs. 3, 8). Shoreface strata overlying the MFI coarsen and shallow upward into deltaic and paralic facies. The disconformities (D1–D4) that bound each sequence show evidence of conspicuous deepening and are composite in nature, representing transgressive surfaces coalesced onto sequence boundaries (Rogers and Kidwell 2000). See figure 7 for locations of sections 1–6. The mid-Judith discontinuity (MJD) correlates with the base of the Woodhawk Member.

ters are exposed (fig. 1). Complete exposures of the McClelland Ferry Member can be readily accessed along south-facing ridges bordering the left bank of the Missouri River from McClelland Ferry to Coal Ridge. Shallow reverse faults carry blocks of the member to the surface near Powerplant Ferry Road (47°43′40.5″N, 108°55′6.8″W) and Heller Bottom (47°44′8.48″N, 108°52′13.7″W). The mudstone-dominated Coal Ridge Member can be traced in surface exposures from the western edge of the type area, where the base of the unit caps ridges along Dog Creek and Birch Creek (fig. 1), downstream to the vicinity of Grand Island (47°41′53.5″N, 108°48′5.9″W), where the upper ~10 m of the unit crops out at river level (fig. 1). Complete sections of the Coal Ridge Member extend from Coal Ridge downstream to Woodhawk Bottom. Both members are readily identified in spontaneous potential and resistivity logs throughout north-central Montana (Rogers 1998; fig. 12).

Strata of the ~70-m-thick McClelland Ferry Member have been interpreted previously as fluvial, floodplain, and coastal mire facies that accumulated landward of the prograding Parkman Sandstone Member during regression of the Claggett Sea (Rogers 1998; Rogers and Kidwell 2000). The basal contact is the boundary between the Parkman Sandstone Member and overlying paralic facies (figs. 3, 4). A bed of lig-

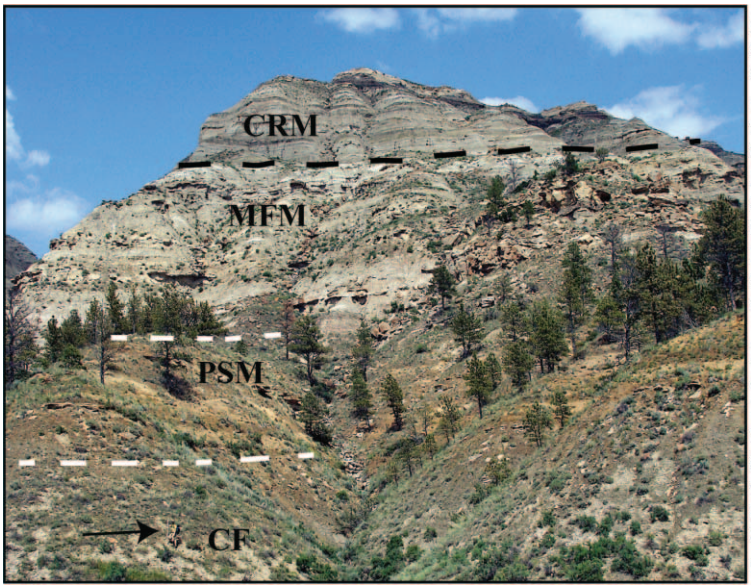


**Coal Ridge Member (CRM):** mudstone-dominated alluvial succession (channel/floodplain ratio 0.51), somber dark gray to olive-green smooth slopes, thinner more lenticular sandstone bodies characterized by rill weathering, fine-grained, relatively enriched in mafic rock fragments and plagioclase, smectite content > kaolinite content, extraformational clasts, general southeast paleoflow (108°), carbonaceous and hydromorphic, evidence of tidal influence, abundant beds of lignite and ironstone, abundant bentonite beds, abundant fossils (plant, invertebrate, vertebrate), including microfossil bonebeds.

**McClelland Ferry Member (MFM):** sandstone-dominated alluvial succession (channel/floodplain ratio 1.13), light gray to pale yellow blocky stairstep-like exposures, thick multistory sandstone bodies, sheet geometries, fine- to medium-grained, relatively enriched in quartz, kaolinite content > smectite content, general southeast paleoflow (129°), abundant orange oxidized concretions, rare bentonite beds, fossils present but less common than in CRM.

**Figure 11.** Comparison of new McClelland Ferry (MFM) and Coal Ridge (CRM) Members of the Judith River Formation at reference section 91-JRT-8 (fig. 3). Position of mid-Judith discontinuity is marked by black dashed line. Contacts separating the Parkman Sandstone Member (PSM) from underlying Claggett Formation (CF) and overlying McClelland Ferry Member are obscured by vegetation and weathered slopes and are thus approximated (white dashed lines). Arrow points to person for scale.

nite overlies the contact in reference section 92-JRT-15, and a bed of fluvial sandstone with tidal indicators caps the Parkman Sandstone Member in 91-JRT-8. The basal contact shows no evidence of significant erosion or prolonged hiatus. The contact separating the McClelland Ferry Member from the overlying Coal Ridge Member coincides with the aforementioned lithologic discontinuity that effectively bisects the 91-JRT-8 stratotype. This discontinuity corresponds with an abrupt up-section shift from sandstone-dominated (McClelland Ferry) to mudstone-dominated (Coal Ridge) strata. Additional distinctions developed across the McClelland Ferry–Coal Ridge contact are detailed below.

Strata of the ~90-m-thick Coal Ridge Member have been interpreted previously as a coastal plain alluvial succession that accumulated landward of backstepping shorelines during transgression of the Bearpaw Sea (Rogers 1994, 1998; Rogers and Kidwell 2000). The Coal Ridge Member thins eastward by interfingering with shallow marine sandstones of the Woodhawk Member (fig. 10). The upper contact of the Coal Ridge Member in 91-JRT-8 separates massive carbonaceous mudstone below from overlying marine siltstones and shales of the Bearpaw Formation. A thin (<1 m) layer of disarticulated oyster shells marks the contact. Downstream from Sturgeon Island (47°48′12.7″N, 109°4′55.3″W), the Coal Ridge Member interfingers with marine sandstones of the Woodhawk Member.

## The Mid-Judith Discontinuity Revisited

***General Considerations and Distinctions.*** Reference section 91-JRT-8 includes a distinctive lithologic discontinuity in facies architecture from a sandstone-dominated to a mudstone-dominated alluvial record, herein referred to as the mid-Judith discontinuity, positioned approximately mid-unit within the Judith River Formation (figs. 3, 5*A*, 5*C*). This widespread discontinuity separates the newly recognized McClelland Ferry Member (below) from the Coal Ridge and Woodhawk Members (above) throughout the Judith River Formation type area (fig. 11). Rogers (1993, 1995, 1998) initially identified this discontinuity and explored many of its distinguishing characteristics in a regional study of the stratigraphy and taphonomy of the Campanian clastic wedge within Montana. The transition can be closely approximated in many surface exposures, as in reference section 91-JRT-8 (fig. 5), but is best expressed and most readily mapped in subsurface data sets, where it is identified by an abrupt shift to the shale baseline in spontaneous potential logs and a coincident drop in resistivity. The transition is evident

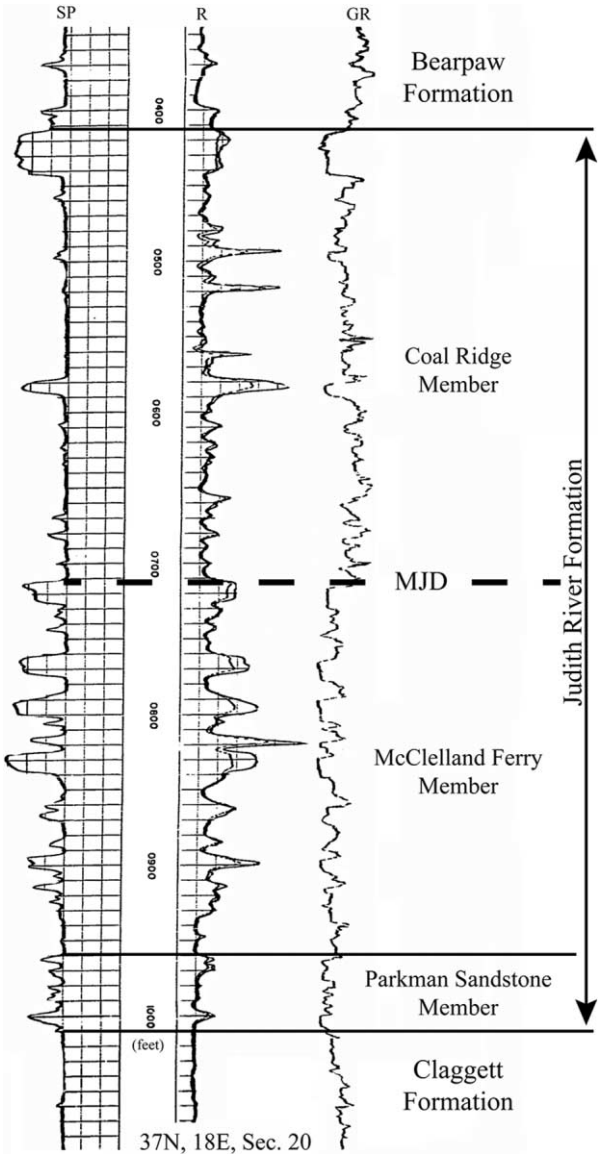


**Figure 12.** Wireline logs spanning the full thickness of the Judith River Formation in the vicinity of Havre, Montana. The abrupt shift in alluvial architecture that defines the mid-Judith discontinuity (MJD) is readily identified in spontaneous potential (SP), resistivity (R), and gamma ray (GR) logs and coincides with an up-section shift to a mudstone-dominated alluvial succession. This subsurface signature can be identified in wireline logs throughout north-central Montana and in southern Alberta and Saskatchewan.

but usually less clearly defined in gamma logs, where it is marked by a right-direction API shift consistent with elevated gamma radiation in the finer-grained Coal Ridge Member (fig. 12).

Several well logs within the type area that are in close proximity to reference section 91-JRT-8 were studied to clarify the position of the mid-Judith discontinuity relative to Formation contacts. Its position above the base of the Judith River Formation can vary among well logs by a few meters, but on average it occurs ~89 m above the base of the Parkman Sandstone Member. Well log data in conjunction with thickness data from outcrops further indicate that the mid-Judith discontinuity can be correlated from the alluvial record in 91-JRT-8 in the western portion of the type area to the approximate base of the of the lowermost backstepping sequence of the new Woodhawk Member in the eastern sector of the type area (Rogers 1998).

The discontinuity is most clearly delimited by the packaging of alluvial sandstones and mudstones. Fluvial sandstone bodies dominate the alluvial succession below the discontinuity (fig. 11), with channel/floodplain ratios in individual sections of the McClelland Ferry Member ranging from 0.88 to 2.70 (median 1.13). Sandstone bodies below the discontinuity crop out as distinct, blocky ledges and are fine- to medium-grained, pale yellow to gray, and sheet-like in geometry. Intraclast lag deposits of ironstone and claystone pebbles are common, as are stacked sets of high-angle trough and tabular cross-bedding. Many of the thicker channel bodies in the McClelland Ferry Member are multistoried, and meter-scale orange-oxidized calcareous concretions are relatively abundant. Paleocurrents derived from medium- to large-scale cross-bed sets ($n = 75$) in the McClelland Ferry Member yield a vector mean of 129° (fig. 13).

In contrast, above the discontinuity, overbank facies dominate the alluvial succession of the Coal Ridge Member (fig. 11), with channel/floodplain ratios ranging from 0.39 to 0.84 (median 0.51). Sandstone bodies here are typically fine grained and weather as rilled light gray slopes. Carbonaceous drapes are common on foresets, toesets, and set boundaries, and comminuted carbonaceous debris is widely disseminated. Trough cross-bedding and lateral accretion deposits are common, as are thin centimeter-scale ironstone beds. Paleocurrents derived from medium- to large-scale cross-bed sets ($n = 66$) in the Coal Ridge Member yield a vector mean of 108° (fig. 13). The lateral continuity of sandstone bodies positioned above the discontinuity is difficult to gauge precisely because of the overall muddy nature of the Coal Ridge Member, but they appear to be more localized and lenticular than their distinctly ledgy and sheet-like counterparts below in the McClelland Ferry Member. The thickness of individual fluvial sandstone bodies varies significantly across the mid-Judith discontinuity ($P \leq 0.02$, Mann-Whitney $U$ and Kolmogorov-Smirnov test). The median thickness of 40 sandstone bodies below

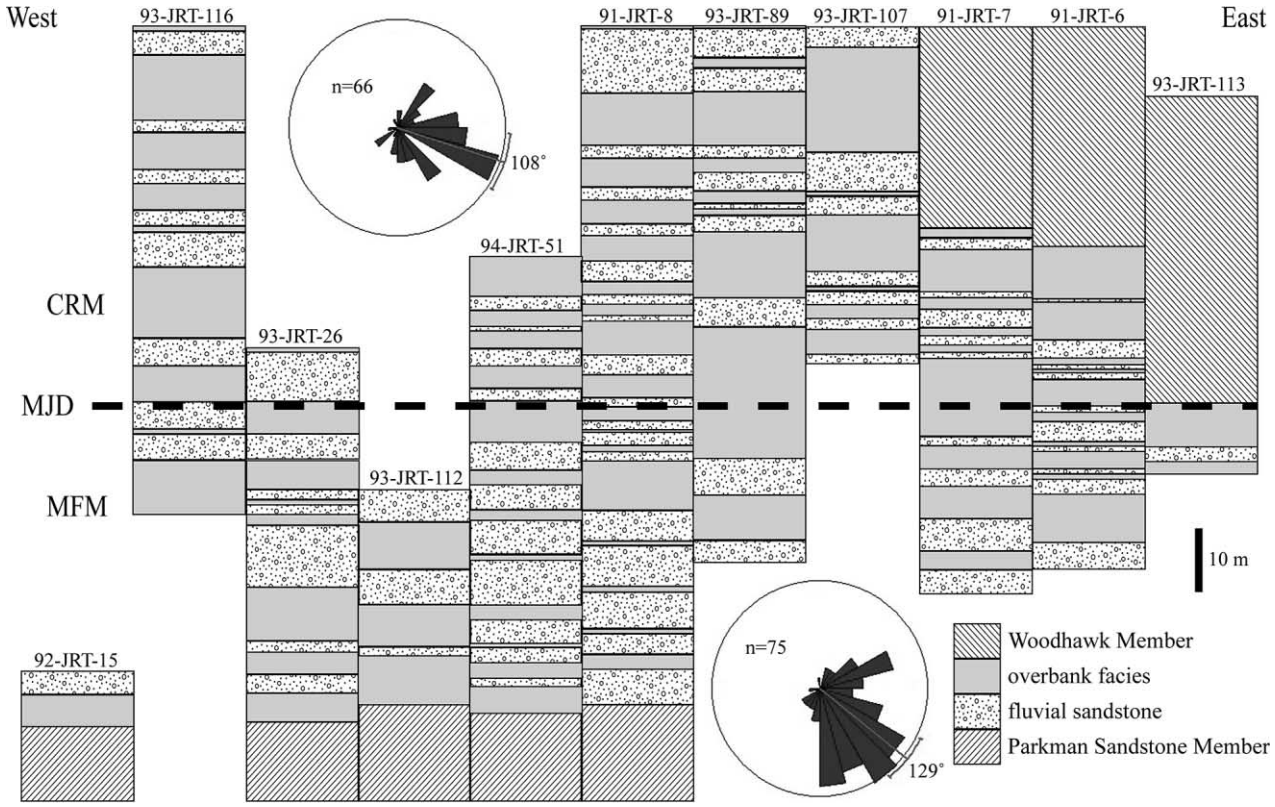


**Figure 13.** The thickness of individual fluvial sandstone bodies varies significantly across the mid-Judith discontinuity (MJD; dashed line; $P \leq 0.02$, Mann-Whitney *U*-test and Kolmogorov-Smirnov test). The median thickness of 40 sandstone bodies below the discontinuity in the McClelland Ferry Member (MFM) is 5.3 m, and that of 43 sandstone bodies above in the Coal Ridge Member (CRM) is 3.35 m; the channel/floodplain ratio declines from 1.13 below to 0.51 above. Fluvial paleocurrents have a general southeast flow direction on both sides of the MJD.

the discontinuity is 5.3 m, contrasted with 3.35 m above (43 sandstone bodies; fig. 13).

The nature of overbank facies also varies across the discontinuity. Overbank facies in the McClelland Ferry Member, lying between the basal paralic deposits and the discontinuity, are generally gray-green to tan mudstones and siltstones and show abundant evidence of rooting and pedogenesis. In contrast, overbank facies arrayed above the discontinuity in the Coal Ridge Member are generally dark gray to olive green in color and are enriched in carbonaceous debris. Evidence of pedogenesis is still common above the discontinuity, but soils are hydromorphic and interspersed with numerous beds of dark gray to black lignite and orange-brown ironstone (Rogers 1998).

Several additional lithologic and paleontologic attributes distinguish facies above and below the mid-Judith discontinuity, as noted in earlier reports (Rogers 1993, 1998; Rogers and Kidwell 2000; Rogers and Brady 2010). Above the discontinuity in the Coal Ridge Member, these include (1) localized concentrations of extraformational pebbles in sandstone bodies; (2) evidence of a shallow water table and tidal influence in paralic facies; (3) a higher frequency of bentonite beds; and (4) a dramatic increase in both invertebrate (freshwater mollusks) and vertebrate fossil occurrences, in particular vertebrate microfossil bonebeds. Sahni (1972) also recognized the shift in the relative abundance of fossils in the Judith River Formation, noting that the upper part of the Formation was more fossiliferous. The dominant lithologies among extraformational clasts are chert, quartzite, hornfels, and vein quartz, all occurring as well-rounded pebbles. Rounded pebbles of felsic plutonic and volcanic rock are also present. The occurrence of these extraformational pebbles is limited to basal lag deposits in fluvial sandstone bodies positioned approximately 10–15 m above the discontinuity.

Evidence of a shallow water table and tidal influence is widespread above the discontinuity in the Coal Ridge Member (Rogers 1998). Hydromorphic

conditions are consistent with the overall abundance of carbonaceous debris in both floodplain and channel deposits, including numerous discrete beds of lignite. With the exception of the uppermost interval of lignite deposits in the Coal Ridge Member, which can be tracked along the same horizon throughout the available outcrop belt, sulfur-bearing lignite beds above the discontinuity appear to track coastal environments that were situated up to 10 km inland of the advancing shorelines of the Woodhawk Member and thus are a diachronous facies linked to the westward transgression of shallow marine facies (fig. 10). Wetland facies with shells of freshwater mollusks (freshwater lakes) are also notably abundant above the discontinuity. Fluvial facies immediately inland of the transgressing Woodhawk Member contain tidal indicators, such as clay- and carbon-draped foresets (sometimes distinctly paired), inclined heterolithic stratification, and rare brackish fauna, including fossil logs with *Teredolites* borings (Rogers 1998).

Beds of altered volcanic ash also show a distinct distribution across the discontinuity. Only one bentonite bed has been identified in the McClelland Ferry Member, in contrast to four above in the Coal Ridge Member (see fig. 3, section 91-JRT-8). The increased frequency of bentonite beds above the discontinuity might reflect more frequent explosive volcanic activity in the region, but preferential preservation under the more aggrading conditions in the Coal Ridge Member cannot be ruled out, given the greater preservation of low-energy overbank deposits.

Fossils of vertebrates, invertebrates, and plants are well represented throughout the Judith River Formation, including the marine Woodhawk Member, but fossils of all types are most abundant in terrestrial strata of the Coal Ridge Member. The distinct increase in fossil occurrences, particularly of vertebrate microfossil bonebeds, probably reflects the fortuitous combination of highly productive coastal wetland ecosystems and favorable chemistry in the burial environment (Rogers and Kidwell 2000; Rogers and Brady 2010). Vertebrate microfossil bonebeds are multi-individual accumulations of disarticulated and dissociated vertebrate hardparts dominated by elements in the millimeter to centimeter size range (≥75% of bioclasts ≤5 cm maximum dimension; Eberth et al. 2007). Conservative reconstructions suggest that microfossil bonebeds in the Judith River Formation may preserve many tens of thousands of vertebrate fossils, although the majority are unidentifiable millimeter-scale fragments. Taphonomic and sedimentologic data are consistent with the in situ accumulation of skeletal debris via attritional mortality in long-lived aquatic ecosystems. Vast quantities of resilient vertebrate hardparts, invertebrate shell debris, and plant material accumulated in these wetland facies, indicating the diversity and abundance of life in the lush coastal plain environments represented by facies of the Coal Ridge Member. Mobile channel belts apparently reworked and locally redeposited preexisting concentrations of fossil debris from floodplains, generating channel-hosted vertebrate microfossil assemblages (Rogers and Kidwell 2000; Rogers and Brady 2010). Geochemical data indicate that some of the reworked fossil concentrations may have already been stabilized by early diagenetic infilling and replacement before exhumation (Rogers and Kidwell 2000; Rogers et al. 2010).

***Mineralogical Trends.*** Petrographic examination of 12 fluvial sandstone bodies spanning the mid-Judith discontinuity in reference section 91-JRT-8 reveals framework grain composition and cementation histories. Sandstones are composed primarily of quartz (24%–63%), volcanic rock fragments (16%–46%), feldspar (4%–20%), and chert (2%–25%), and most can be categorized as litharenite or feldspathic litharenite, using McBride's (1963) classification (fig. 14). Trace framework constituents include biotite, mucscovite, apatite, monazite, zircon, and detrital carbonate grains. Sandstones from 91-JRT-8 are also texturally submature, with grain size ranging from fine to medium and grain shape ranging from angular to subrounded. Volcanically derived lithic grains are present in all samples and tend to be larger and more rounded than monomineralic counterparts. Rare grains of well-rounded quartz exhibiting dust lines and quartz overgrowths are present both above and below the discontinuity. Foliated metamorphic and sedimentary rock fragments are also represented.

Overall, few differences are evident across the mid-Judith discontinuity in the sand-sized fraction. Sandstones in the McClelland Ferry Member are somewhat more enriched in quartz (fig. 15*A*, 15*B*), and sandstones in the Coal Ridge Member above the discontinuity are in general more enriched in mafic volcanic rock fragments (fig. 15*C*). Sandstones above the discontinuity are also notably enriched in plagioclase, with some showing a fourfold increase in the abundance of albite (fig. 15*D*). The sandstone body that coincides most closely with the discontinuity in 91-JRT-8 (see fig. 3) is relatively rich in quartz (but not the most quartzose sandstone encountered) and contains abundant grains of authigenic dolomite (fig. 15*E*, 15*F*) that are often rhombohedral and almost always rimmed with iron oxide cement.

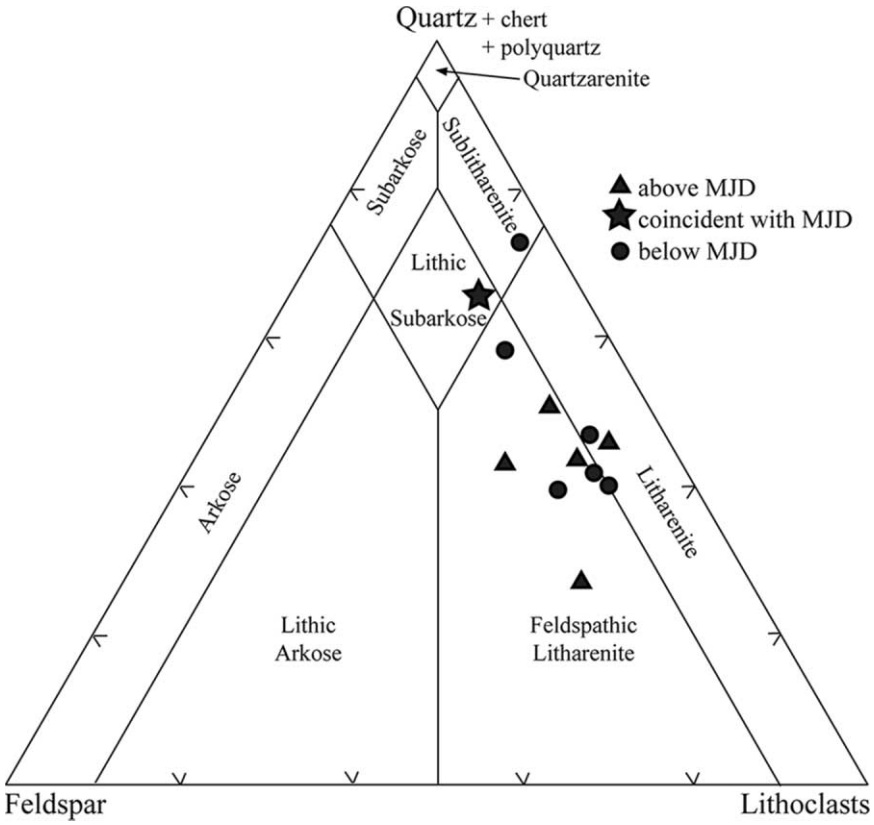


**Figure 14.** Most fluvial sandstones in the Judith River Formation can be categorized as litharenite/feldspathic litharenite (McBride 1963), containing mixtures of quartz (24%–63%), volcanic rock fragments (16%–46%), feldspar (4%–20%), and chert (2%–25%). Sandstones below the discontinuity (circles) are somewhat more enriched in quartz. Sandstones above the discontinuity (triangles) are on average more enriched in mafic volcanic rock fragments and plagioclase, with some showing a four-fold increase in the abundance of albite. The sandstone body that intersects the mid-Judith discontinuity in 91-JRT-8 (star) is relatively rich in quartz and contains abundant authigenic dolomite. Ternary diagram constructed with Delta Plot (John 2004).

Matrix and cement composition were also examined. Two sandstone samples present below the discontinuity and four above it are cemented by calcite. There is widespread replacement of mineral grains and lithic fragments by calcite, especially where calcite is the predominant cementing agent, and many of these grains exhibit etched margins with clear evidence of corrosion. Sandstones lacking calcite cement typically have a grungy matrix of crushed and deformed lithic clasts (fig. 15*C*), and this pseudomatrix (Dickinson 1970) makes it difficult to identify individual lithic clasts. Interstitial spaces are also filled locally with microcrystalline silica cement, clay, and, more rarely, fluorite cement (fig. 15*F*). Most significantly, the quartz-rich sandstone body most closely associated with the discontinuity in reference section 91-JRT-8 has a unique petrologic signature, with abundant authigenic dolomite and pervasive iron oxide cement (fig. 15*E*, 15*F*). Primary porosity is also notably developed in this particular sandstone, perhaps indicating early cementation by authigenic iron oxide and carbonate and the persistence of primary void space.

Clay content was also determined for 86 samples that span the mid-Judith discontinuity in reference section 91-JRT-8 (fig. 16). X-ray diffraction analyses indicate that four clay minerals are consistently represented in the section: kaolinite, smectite, illite, and chlorite. Numerous nonclay minerals were also identified in the clay-sized fraction, including goethite, quartz, orthoclase, albite, anorthite, calcite, and dolomite. The weight-percent abundances of clay minerals are plotted in figure 16. Kaolinite and smectite are abundant throughout reference section 91-JRT-8 and together comprise up to 75 wt% of most samples. Kaolinite is most abundant within sandstones. Smectite, illite, and chlorite clays tend to be more abundant in finer-grained siltstones and

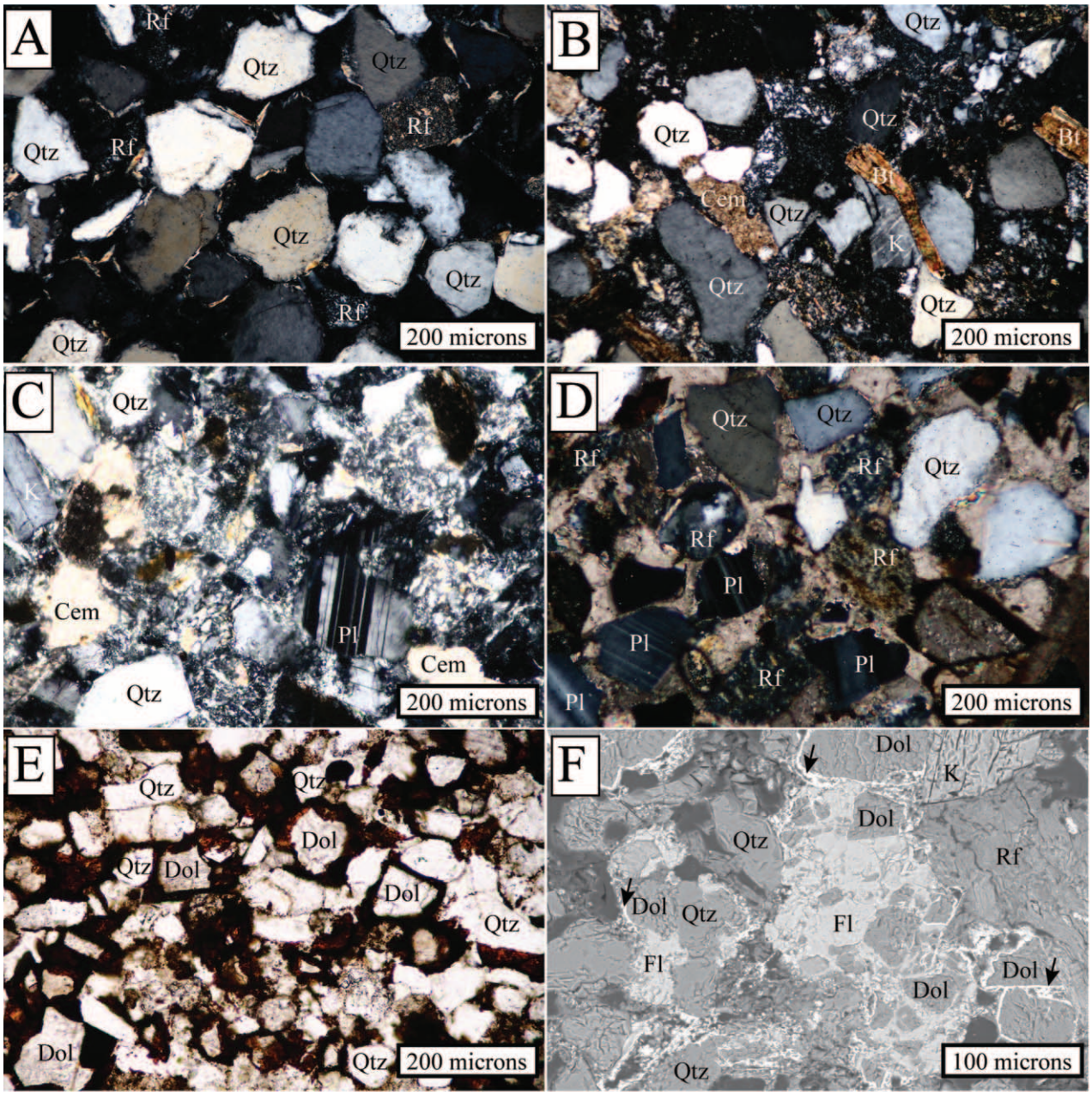


**Figure 15.** Photomicrographs of Judith River Formation fluvial sandstones, showing trends in sandstone petrology and cement content across the mid-Judith discontinuity (MJD). *A*, Quartz-rich (Qtz) sandstone ~60 m below the MJD, with relatively few rock fragments (Rf) and abundant sericite alteration rims; crossed polars. *B*, Sandstone ~50 m below MJD, characterized by felsitic rock fragments, biotite grains (Bt), potassium feldspar grains (K), and patchy calcite cement (Cem); crossed polars. *C*, Sandstone ~10 m above MJD exhibiting pseudomatrix of crushed mafic and felsitic rock fragments and plagioclase (Pl), potassium feldspar (K), and quartz (Qtz) grains; crossed polars. *D*, Calcite-cemented sandstone ~40 m above MJD with abundant plagioclase grains associated with quartz grains and rock fragments; crossed polars. *E*, Sandstone positioned at the level of MJD characterized by pervasive iron oxide cement and abundant coated detrital dolomite grains (Dol). *F*, Backscatter electron image illustrating occurrence of patchy fluorite cement (Fl) in same sandstone body in association with quartz, dolomite, potassium feldspar, and weathered rock fragments. Thin bright bands coating grains represent iron oxides (arrows).

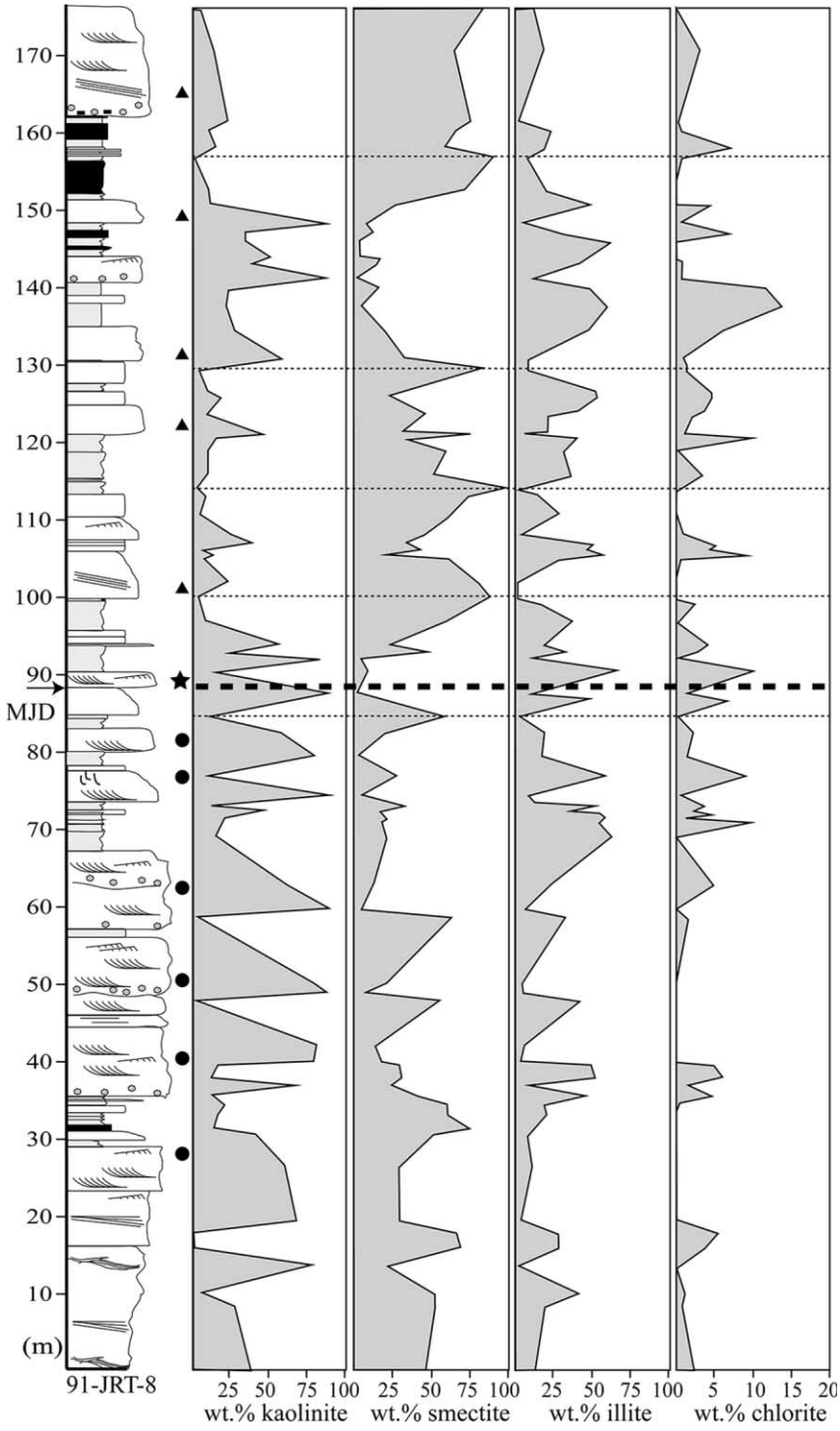


**Figure 16.** Weight percent abundance of clay minerals varies in reference section 91-JRT-8 in relation to facies context and position above or below the mid-Judith discontinuity. Kaolinite and smectite are abundant throughout the section (together representing up to 75 wt%). Kaolinite is most abundant within sandstones, whereas smectite, illite, and chlorite clays (note change in scale) are more abundant in siltstones and mudstones. The relative abundance of kaolinite decreases significantly across the mid-Judith discontinuity (thick dashed line), whereas the relative abundance of smectite increases. Circles, triangles, and star indicate sandstone samples included in point counts in figure 14. Thin dotted lines mark the positions of bentonite beds.

mudstones. The relative abundance of kaolinite decreases significantly across the discontinuity, whereas the relative abundance of smectite increases. No change in the average relative abundances of illite and chlorite are evident (fig. 16). When all samples from all lithofacies are compared across the discontinuity (43 below, 44 above), significant distinctions in both kaolinite and smectite content are well supported at the 99% confidence interval (kaolinite, $P \leq 0.009$; smectite, $P \leq 0.01$; Mann-Whitney *U*-test). Controlling for lithofacies context, kaolinite is significantly more abundant in sandstones below the discontinuity ($n = 14$) than in sandstones above it ($n = 14$; $P \leq 0.002$: Mann-Whitney *U*-test). The prevalence of kaolinite below the discontinuity imparts a decidedly pale cast to the McClelland Ferry Member, with exposures characterized by shades of light gray and pale yellow. In contrast, smectite-rich alluvial facies above the discontinuity in the Coal Ridge Member are generally a somber gray and olive-green color, augmented with the dark gray and black banding of abundant carbonaceous mudstones and lignite beds.

## New $^{40}Ar/^{39}Ar$ Ages from the Judith River Formation Type Area

***Bentonite Stratigraphy.*** Altered volcanic ash beds (bentonites) are relatively common throughout the Upper Cretaceous section in the Montana portion of the Western Interior Basin. Nearby volcanic centers in Montana linked to explosive events and airfall ash during the Late Cretaceous include the Elkhorn Mountains Volcanics and the Adel Mountains Volcanics (Viele and Harris 1965; Smedes 1966; Tilling et al. 1968; Thomas et al. 1990; Rogers et al. 1993; Roberts and Hendrix 2000; Foreman et al. 2008). The new radioisotopic ages reported here are the first derived from bentonites collected within the confines of the Judith River Formation type area. The only previously published radioisotopic ages for the Judith River Formation within Montana were derived from two bentonite beds collected from low in the formation far to the north in Kennedy Coulee, near Rudyard, Montana (Goodwin and Deino 1989).

New ages are reported here from three bentonite beds (figs. 3, 10). Bentonite bed ST1-03 (47°45′37.2″N, 109°19′46.9″W) occurs 84.5 m above the base of the Judith River Formation in reference section 91-JRT-8 in alluvial sediments of the McClelland Ferry Member, immediately below the mid-Judith discontinuity. Bentonite bed WHB1-11 (47°44′57.9″N, 108°56′42.6″W) occurs 108 m below the top of the Judith River Formation in the vicinity of reference section 91-JRT-12 in alluvial sediments of the McClelland Ferry Member, ~10 m below the mid-Judith discontinuity. Bentonite bed PPF1-03 (47°43′28.7″N, 108°56′37.3″W) is at the base of the Bearpaw Formation, approximately 5 m above the top of the Judith River Formation, and was sampled at the top of a ridge 2.5 km to the southeast of reference section 91-JRT-12 (fig. 10). All three bentonite beds exhibit popcorn weathering in outcrop, indicating significant smectite clay content, and all three preserve euhedral grains of sanidine, biotite, and other volcanogenic crystals at their base. ST1-03 and WHB1-11 are only locally exposed and are thin (≤15 cm thick) compared with PPF1-03, which is a prominent bed up to 30 cm thick that can be traced throughout much of the type area. The stratigraphic positions of ST1-03, WHB1-11, and PPF1-03 are indicated in figures 3 and 10.

***$^{40}Ar/^{39}Ar$ Results.*** Summary $^{40}Ar/^{39}Ar$ analytical data are presented in figure 17 (related data in table S1, available online or from the *Journal of Geology* office). Ten sanidine phenocrysts from sample ST1-03 yielded a weighted-mean $^{40}Ar/^{39}Ar$ age of 76.24 ± 0.18 Ma (1$\sigma$ internal error; ±0.22 Ma 1$\sigma$ full external error), 12 sanidine phenocrysts from sample PPF1-03 yielded 75.21 ± 0.12 Ma (± 0.17 Ma), and 30 sanidine phenocrysts from sample WHB1-11 yielded 76.17 ± 0.07 Ma (± 0.14 Ma).

Recent astronomical recalibration of the age of Fish Canyon sanidine standard by Kuiper et al. (2008), used herein, requires recalculation of prior reported $^{40}Ar/^{39}Ar$ ages (e.g., Roberts et al. 2013). With regard to legacy ages in the Judith River Formation, the original $^{40}Ar/^{39}Ar$ analyses of the Kennedy Coulee bentonites yielded ages of 78.5 ± 0.2 Ma for sanidine in the lower bentonite and 78.2 ± 0.2 Ma for sanidine in the upper bentonite (Goodwin and Deino 1989), which after recalculation are 79.5 ± 0.2 and 79.1 ± 0.2 Ma, respectively. Note that calibration work on the Fish Canyon sanidine standard continues (e.g., Phillips and Matchan 2013; Renne 2013), but the changes are likely to be less than a few tenths of a percent, and $^{40}Ar/^{39}Ar$ ages can always be recalculated if a consensus is reached within the geochronological community as to the canonical age of this standard.

## Discussion

***Age and Correlation of the Mid-Judith Discontinuity.*** New radioisotopic ages reported here (fig. 17) indicate that the mid-Judith discontinuity formed at approximately 76.2 Ma, shortly after or roughly

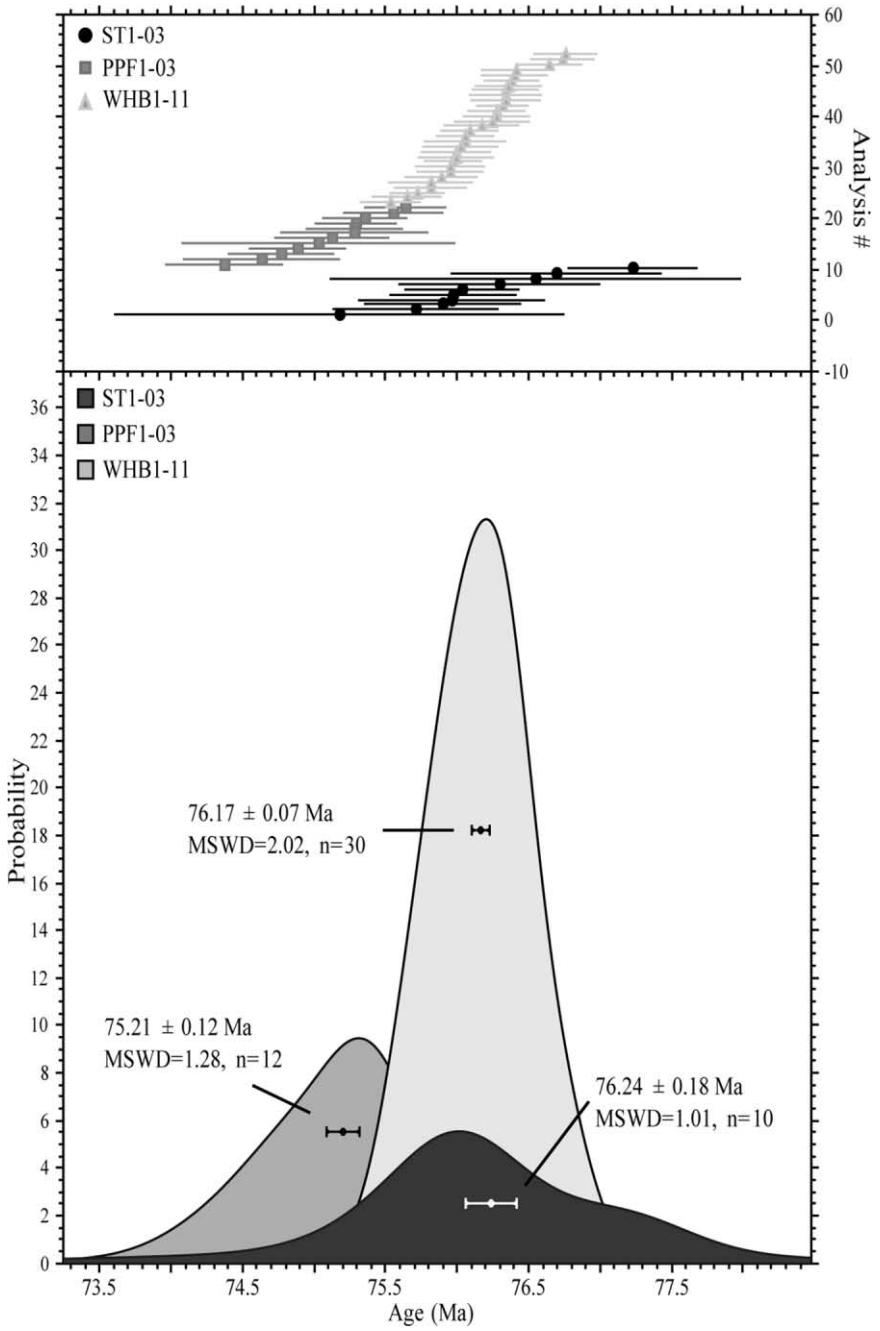


**Figure 17.** Age probability density plots for single-crystal sanidine $^{40}Ar/^{39}Ar$ age determinations from bentonite beds ST1-03, PPF1-03, and WHB1-11 (see figs. 3, 10) sampled from the type area of the Judith River Formation in north-central Montana (Upper Missouri River Breaks National Monument). Weighted mean ages of the three populations are indicated, with errors reported at 1$\sigma$.

coincident with emplacement of the ST1-03 (76.24 ± 0.18 Ma) and WHB1-11 (76.17 ± 0.07 Ma) bentonites. Rock accumulation rates of Judith River strata beneath the discontinuity can be approximated by considering the recalibrated legacy ages from Kennedy Coulee with new radioisotopic age data from ST1-03 and WHB1-11. Basal exposures of the Judith River Formation in Kennedy Coulee range in age from ~79.5 to 79.1 Ma. As a clastic tongue, the Judith River Formation thickens westward from the type area toward Kennedy Coulee, and well logs in that general vicinity indicate that Judith River strata

beneath the discontinuity span at least 125 m. Age data and thickness estimates for the lower Judith River section (Parkman Sandstone and McClelland Ferry Members combined) thus suggest rock accumulation rates on the order of ~3.8 cm/1000 yr.

Deposition of the Judith River Formation ceased in north-central Montana before 75.21 ± 0.12 Ma, which is the age of the PPF103 bentonite at the base of the overlying Bearpaw Formation. On the basis of this new age and the ~76.2 Ma age of the mid-Judith discontinuity, the ~90-m section between the discontinuity and the Bearpaw Formation (the alluvial Coal Ridge Member and laterally equivalent marine Woodhawk Member) accumulated over roughly 1.0 Ma, with an average rock accumulation rate of ~9 cm/1000 yr. Rock accumulation rates thus more than double across the discontinuity, and the three high-frequency sequences that compose the Woodhawk Member each have cycle durations on the order of 0.3–0.4 Ma, making them fourth-order packages.

Correlation of the mid-Judith discontinuity northward provides a means of establishing stratigraphic age control for several important fossil localities, assuming that this turnaround from regressive, prograding sedimentation to transgressive and strongly aggradational sedimentation provides a reasonable time plane. Exposures of the Judith River Formation in the Havre region preserve abundant vertebrate microfossil bonebeds and have yielded well-preserved dinosaur egg clutches (Clouse and Horner 1993; Horner 1999). The Havre badlands are approximately due north along strike of the western edge of the Judith River Formation type area, and the strata exposed near Havre readily compare with the stratigraphic succession in the type area. The Judith River section in the Havre region spans ~180 m, and the discontinuity is well expressed approximately midunit in subsurface logs (figs. 11, 18). The lower part of the section is dominated by fluvial sandstone sheets, and most documented fossil occurrences—including the dinosaur egg clutches—occur in strata above the discontinuity. These are thus between 76.2 and 75.2 Ma in age and lie within the new Coal Ridge Member of the Judith River Formation.

Vertebrate fossil localities ~60 km farther to the west, in the vicinity of Rudyard (Kennedy Coulee), can also be contextualized relative to the mid-Judith discontinuity. Outcrop and subsurface data in that area indicate that only the lower portion of the Judith River Formation is exposed (Parkman Sandstone Member and new McClelland Ferry Member). The discontinuity is discernible in subsurface logs north of the border in southern Alberta, where more expansive subsurface sections of equivalent strata (Belly River Group) are readily available. All fossil occurrences in the Kennedy Coulee study area (e.g., Clemens and Goodwin 1985; Montellano 1991; Schott et al. 2010) can thus be confidently placed below the mid-Judith discontinuity in rocks older than ~76.2 Ma but probably younger than ~79.5 Ma.

***Origin and Significance of the Mid-Judith Discontinuity: A Maximum Regressive Surface.*** The mid-Judith discontinuity is an apparently conformable, readily mapped break in lithology embedded approximately mid-unit within the Judith River Formation. It is a widespread, readily recognized abrupt change in the nature of the alluvial record, from sandstone- to mudstone-dominated facies suites that contain more abundant fossil vertebrates, more plagioclase and mafic rock fragments in framework sands, more hydromorphic features, with smectitic rather than kaolinitic clays, and that accumulated at rates more than twice as fast. The discontinuity marks a major adjustment of alluvial systems within the basin, from regressive and predominantly progradational deposition below the discontinuity to transgressive and strongly aggradational deposition above it.

Rogers (1998) originally proposed that the mid-Judith discontinuity separated terrestrial deposits that accumulated landward of shorelines that prograded eastward during the Claggett regression from terrestrial facies that accumulated landward of backstepping shorelines during the subsequent Bearpaw transgression, of which the new Woodhawk Member of the Judith River Formation is the leading marine edge. He further suggested that the discontinuity formed in response to a change in the rate of positive accommodation in the Montana portion of the Western Interior foreland basin, presumably in response to tectonic loading of the basin margin. Here we reevaluate this reconstruction of base-level change and bring new data to bear on the question.

With the resolution afforded by subsurface data, the mid-Judith discontinuity can be correlated throughout the Judith River Formation type area in north-central Montana, from fully terrestrial rocks in the western portion of the type area to the approximate base of the marine Woodhawk Member in the eastern sector. This correlation is illustrated by dip-parallel cross section *A*–*A*′ in figure 18, which spans approximately 70 km across the full expanse of the type area. The regional resistivity kick that marks the Eagle/Milk River shoulder, which was previously interpreted as a transgressive surface of erosion (Payenberg et al. 2003), is used here as a subcrop datum throughout north-central Montana and in the southern plains of western Canada. The mid-Judith

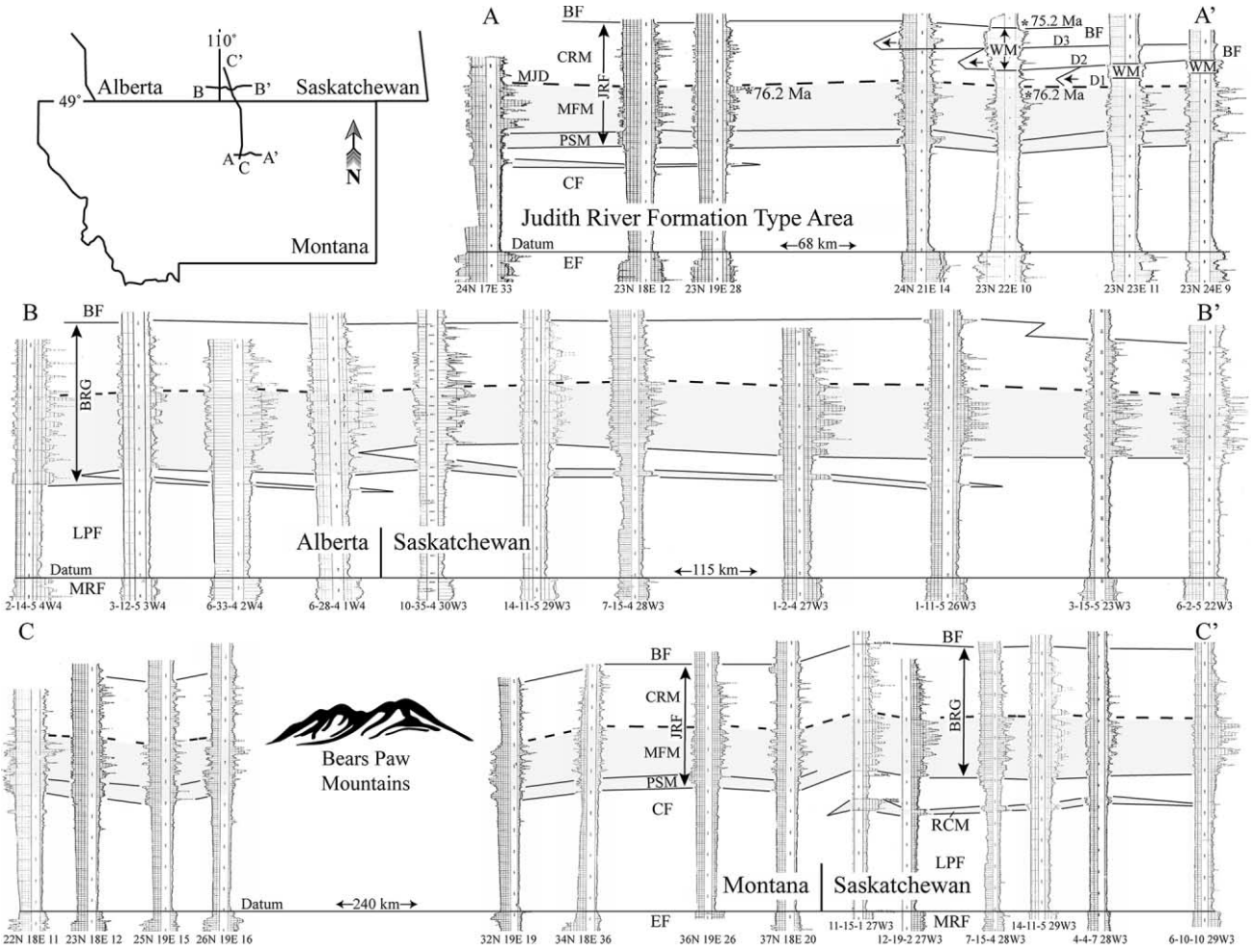


**Figure 18.** Subsurface correlation of the mid-Judith discontinuity (MJD; dashed line), with terrestrial and sandy shallow marine strata below the discontinuity shaded gray. The discontinuity can be correlated across north-central Montana (*A*–*A*′) and northward into southern Alberta and Saskatchewan, Canada (*B*–*B*′, *C*–*C*′), using electric logs (MJ Systems). The regional resistivity kick that marks the Eagle/Milk River shoulder (transgressive surface at top of Eagle Formation [EF] in Montana and Milk River Formation [MRF] and equivalent units in Canada; Payenberg et al. 2003) is used as a subcrop datum in all three cross sections. *A*–*A*′, The MJD can be traced from fully terrestrial rocks in the western portion of the type area to the base of the marine Woodhawk Member in the eastern portion in this dip-parallel section, which spans approximately 70 km across the entire type area. New $^{40}Ar/^{39}Ar$ ages from the Judith River Formation (JRF) type area are shown in their approximate stratigraphic and geographic positions. *B*–*B*′, In this dip-parallel section situated approximately 35 km to the north of the international border, strata below the discontinuity exhibit wireline responses consistent with alluvial deposits dominated by thick and closely spaced sandstone bodies, and those above the discontinuity exhibit responses consistent with fine-grained deposits containing fewer and thinner sandstone bodies. This 115-km-long transect from southeastern Alberta to southwestern Saskatchewan does not extend far enough to the east to intersect rocks equivalent to the Woodhawk Member (WM). *C*–*C*′, Strike-parallel section extending 240 km from the type area of the JRF in north-central Montana to approximately 15 km north of Cyprus Hills Interprovincial Park in southwestern Saskatchewan. The stratal architecture that typifies the JRF in its type area can be correlated with surprisingly little variation in thickness. PSM = Parkman Sandstone Member; MFM = McClelland Ferry Member; CRM = Coal Ridge Member; CF = Claggett Formation; BF = Bearpaw Formation; D1, D2, D3 = disconformities marking bases of depositional sequences of Woodhawk Member (fig. 10); BRG = Belly River Group; LPF = Lea Park Formation (Pakowki Formation equivalent); RCM = Ribstone Creek Member of BRG.

discontinuity essentially parallels this datum, showing remarkably little variation in thickness of intervening strata across this clastic wedge.

A second dip-parallel cross section (B–B′) situated approximately 35 km to the north of the international border and based entirely on well logs exhibits the same basic pattern (fig. 18). Strata below the discontinuity exhibit wireline responses consistent with a record dominated by thick and closely spaced sandstone bodies, and strata above the discontinuity are consistent with a finer-grained section typified by fewer and thinner sandstone bodies. This B–B′ cross section extends for approximately 115 km across the plains of southeastern Alberta and southwestern Saskatchewan. Terrestrial and shallow marine strata below the discontinuity thicken to the west, as would be expected of a clastic wedge prograding eastward (basinward) from western source areas. This cross section does not extend far enough to the east to intersect marine strata correlative with the Woodhawk Member. Here again the mid-Judith discontinuity essentially parallels the subsurface datum, showing general continuity in thickness of the intervening stratigraphic package.

The mid-Judith discontinuity can also be traced for considerable distance along depositional strike, as exemplified by cross section C–C′ in figure 18. This cross section extends from the type area of the Judith River Formation in north-central Montana to approximately 15 km north of Cyprus Hills Interprovincial Park in southwestern Saskatchewan, a distance of ~240 km. The only gap in the correlation occurs across the Bears Paw Mountains, which were emplaced as part of the Central Montana Alkalic Province during the Eocene (Diehl et al. 1983). The same basic stratal architecture that typifies the Judith River Formation in its type area can be correlated northward for at least 240 km with surprisingly little variation in thickness. The ~25-m step-up away from the datum across the Montana-Saskatchewan border coincides with the subsurface expression of the Ribstone Creek Member of the Campanian Belly River Group and likely reflects the impact of this sandstone tongue on compaction of strata between the Eagle/Milk River shoulder and the base of Judith River equivalent strata.

Thus, on the basis of subsurface data sets in north-central Montana and the southern plains of western Canada, the mid-Judith discontinuity spans at least 27,000 km$^2$. The widespread nature of the discontinuity and the strong change in accumulation rates and in facies architecture across it suggest that it reflects a major base level–related adjustment within the foreland basin across north-central Montana and into the southern plains of Canada rather than a local event or a change in sediment supply alone, such as from climate change. Given its spatial extent, the discontinuity is also unlikely to reflect autogenic processes, such as variable avulsion frequency: intrinsic processes of fluvial systems generally operate on more local scales, and their signature would be expected to be both more clustered from a stratigraphic perspective and more diachronous in nature (e.g., Hajek and Heller 2012; Hajek et al. 2012). There is evidence for climate change in correlative strata of the Belly River Group to the north in Canada (Eberth et al. 2013), with conditions evolving from a warm and seasonally dry paleoclimate in the Oldman Formation (approximate age equivalent to the McClelland Ferry Member) to a warm and more consistently wet climatic regime in the overlying Dinosaur Park Formation (approximate age equivalent to the Coal Ridge Member). A comparable shift in rainfall patterns likely affected contiguous regions of Montana during the Campanian. However, a regional shift to wetter conditions is compatible with only a few of the features that change across the mid-Judith discontinuity, such as the up-section shift to hydromorphic facies. The observed shifts in channel scale, clay mineralogy, framework mineralogy, and increased rate of aggradation would not be predicted by an increase in rainfall alone. Some different or additional form of external forcing of the alluvial system, such as from tectonic subsidence and/or eustasy (specifically a rise), thus seems required.

Correlation of the mid-Judith discontinuity to the base of the Woodhawk Member provides a key constraint for the origin of the discontinuity. Shallow marine sandstones of the Woodhawk Member are juxtaposed upon alluvial facies of the McClelland Ferry Member. This abrupt deepening signals significant addition of accommodation and marine transgression, which then persisted for the duration of Woodhawk Member deposition, as evidenced by the retrogradational pattern of the three high-frequency depositional sequences that form the Woodhawk Member. Terrestrial strata of the Coal Ridge Member above the discontinuity and below the Bearpaw Formation accumulated during deposition of the Woodhawk Member and thus accumulated during the same episode of underfilled accommodation that prompted regional marine transgression. Tidal indicators in Coal Ridge Member facies are further evidence that these strata accumulated synchronous with marine transgression. The pervasive hydromorphic character of this member is also consistent with rising base level in the coastal complex inland of the Woodhawk Member (Wright and Marriott 1993; McCarthy et al. 1999; Plint et al. 2001).

The tectonic context of the Judith River Formation, within the foredeep of an active foreland basin, guides interpretation of the driver of the geologically sudden addition of accommodation. The Campanian was a time of slip along major thrust systems in the fold and thrust belt in northwestern Montana (Sears 2001; Fuentes et al. 2011), and the Bearpaw transgression was the last large-scale flooding event within the basin. Tectonic loading and related flexural subsidence have been argued to be the major driving force behind transgressive-regressive cycles within the Bearpaw Formation in adjacent regions of southern Alberta and Saskatchewan (Catuneanu et al. 1997), and a similar tectonic response would be expected in the Montana portion of the same basin.

An upstream tectonic explanation for the addition of accommodation (sensu Aitken and Flint 1995; Miall 1997; Catuneanu 2006; Eberth and Braman 2012) is consistent with several aspects of the alluvial record spanning the discontinuity. First and foremost, this clastic tongue representing the proximal Two Medicine and more distal Judith River Formations thickens dramatically to the west toward the orogen, as would be predicted in an asymmetrically subsiding foredeep (fig. 2). The geometry of the wedge is consistent with flexural subsidence as a first-order control on accommodation and sedimentation patterns during the Campanian. In addition, petrologic data indicate that the delivery of clastic detritus evolved across the discontinuity, with an increase in extraformational lithic clasts, which is consistent with the tectonic reorganization of source areas and sedimentary delivery systems. A pulse of extraformational pebbles appears in the basin fill shortly after formation of the discontinuity, and an increased flux of mafic volcanic rock fragments and plagioclase is evident in sandstones above the discontinuity (fig. 15). The increased frequency of bentonite beds above the discontinuity is also consistent with a tectonic link to subsidence and the addition of accommodation, assuming magmatic activity accompanied diastrophic events in the hinterland, but their increase might also be an epiphenomenon of higher preservation potential linked to overall higher rates of aggradation.

Finally, there is the question of how to categorize this regional stratigraphic discontinuity in terms of base-level cycles and sequence stratigraphic models (Rogers 1998; Rogers and Kidwell 2000). One feature absent from the mid-Judith discontinuity is evidence of significant erosion of underlying strata, such as channel incisions of exceptional depth or low-angle beveling that might be detected at the scale of our large badland-type outcrops. There is also no regional evidence of erosion or distal downstepping, at least such as can be recognized in available outcrop and subsurface data: stacking patterns up to this point are apparently simply progradational. The mid-Judith discontinuity also shows no particularly strong evidence of sediment bypass (sensu Holbrook and Bhattacharya 2012). The most closely associated sandstone body exhibits distinctive diagenesis in the form of abundant authigenic dolomite and iron oxide cement, but this could reflect overprinting by the hydromorphic deposits that succeed it. Sandstones along the discontinuity are not especially amalgamated or rich in pebbly debris, such as would suggest a thin, residual record of bypass. Instead, the discontinuity simply marks a pronounced change in facies architecture, specifically a strong reduction in the sandstone/mudstone ratio of alluvial facies, and a shift in detrital composition and authigenic clay composition, coincident with a change in shoreline trajectories from regressive to transgressive and a sharp increase in rates of rock accumulation. These changes are consistent with a change to backstepping.

The discontinuity thus has features that would be expected of the upstream, terrestrial extension of a maximum regressive surface, marking a shift from normal regression to transgression (sensu Helland-Hansen and Gjelberg 1994; Helland-Hansen and Martinsen 1996; Catuneanu 2006; Catuneanu et al. 2011). The mid-Judith discontinuity would correspond to the surface of initial transgression (sensu Posamentier and Vail 1988) further seaward in the basin; in the eastern sector of the Judith River type area, the stratigraphically lowest transgressive surface at the base of the Woodhawk Member (D1; figs. 10, 18) coincides with the mid-Judith discontinuity. Stratigraphic discontinuities with some of the above-mentioned features would also satisfy the definition of a cryptic sequence boundary (sensu Miall and Arush 2001).

***Comparing Low- and High-Accommodation Terrestrial Records across the Mid-Judith Discontinuity.*** Rock accumulation rates show a more than two-fold increase across the mid-Judith discontinuity. This doubling of rock accumulation rates arguably translates to a comparable increase in floodplain aggradation rates in the Coal Ridge Member of the upper Judith River Formation. Classic models of alluvial architecture (e.g., Leeder 1978; Bridge and Leeder 1979; Alexander and Leeder 1987) contend that an increase in aggradation rates in a positive accommodation setting would compel the alluvial record toward (1) enhanced preservation of floodplain fines, (2) diminished channel stacking density, and (3) diminished channel amalgamation and connectivity.

All of these expectations are borne out on a regional scale in alluvial Coal Ridge Member strata above the mid-Judith discontinuity, landward of the shoreface Woodhawk Member (fig. 18). The system responded rapidly and regionally to flexural subsidence in ways predicted both by early models of alluvial architecture and by more recent considerations of terrestrial sequence stratigraphy (Wright and Marriott 1993; Leckie and Boyd 2003; Catuneanu 2006; Tedesco et al. 2010; Colombera et al. 2015). That is not to say that other controls on alluvial architecture, such as climate and various autogenic processes, were not in play. However, it is difficult to downplay the links between the shift in accommodation regimes, marine transgression, and changes in channel stacking patterns in the alluvial Judith River record.

The dramatic increase in floodplain aggradation rate above the mid-Judith discontinuity can also account for the distinct pattern of clay mineral distribution across the discontinuity. The shift from a kaolinite-dominated record below to a smectite-dominated record above is consistent with the expected intensity of weathering in the near-surface burial environment. Diagenesis and the early authigenic formation of clay minerals such as kaolinite would proceed more effectively under conditions of relatively low addition of accommodation and slow net aggradation, because meteoric waters would have more time to effectively flush cations from the system (Chamley 1989; Birkeland 1999; Ketzer et al. 2003; Khidir and Catuneanu 2009). Under this same premise, and with other controls on weathering held relatively constant, the early diagenetic production of kaolinite would be inhibited by the more than two-fold increase in floodplain aggradation rate in the upper Judith River record, especially when coupled with a rising water table, which would impede the flushing of cations. Importantly, the pattern of clay mineral distribution in the Judith River record parallels a significant shift in the channel/floodplain ratio, and so early diagenetic processes would be expected to proceed fastest within permeable sediments such as sandstones (Huggett 1986). Thus, to some degree, the abundance of kaolinite in the McClelland Ferry Member might simply be a function of the abundance of sandstone in the same record. On the other hand, the shift in clay mineralogy is evident in both sandstones and mudstones (fig. 16); thus, facies-specific weathering trends can explain only part of the pattern. A broader control linked to the shift from a low- to a high-accommodation setting and the overall duration of weathering in alluvial sediments thus seems to have been operating, with important implications for the recognition of significant surfaces and stratigraphic intervals in studies of terrestrial sequence stratigraphy, especially those of a cryptic nature (e.g., Miall and Arush 2001; Khidir and Catuneanu 2009).

The abrupt shift in accommodation and alluvial architecture that punctuates the Judith River record is thus marked by a change in clay signatures, which characterize expansive intervals of alluvial strata that accumulated under distinct accommodation regimes on opposite sides of the mid-Judith discontinuity: there is no clay signature of a particular surface or thin (presumably hiatal) interval within this part of the succession. The mid-Judith discontinuity does nonetheless correspond with one unique and localized diagenetic signature: the sandstone body that most closely coincides with the discontinuity in reference section 91-JRT-8 is characterized by abundant authigenic dolomite and distinctive iron oxide cementation (fig. 15*E*, 15*F*). No other sandstone in the section shows comparable precipitation of secondary dolomite and iron oxide, and the early emplacement of authigenic cement is suggested by the retention of primary porosity. The exact time frame of diagenesis is not yet resolved, but it seems reasonable to propose that some degree of subaerial hiatus would have promoted the in situ weathering of magnesium- and iron-bearing minerals and afforded time for the circulation of oxidizing meteoric fluids. In any case, this unique diagenetic signature coincides precisely with a change from prolonged regression to a pulse of marine transgression and a change in the rate of addition of accommodation.

Last, the relative richness of the bioclastic record preserved in the high-accommodation Coal Ridge Member parallels previous observations in other basins and other depositional settings that compare aspects of fossil preservation and accommodation (e.g., Kidwell 1988, 1993*a*, 1993*b*; Eberth et al. 2001). The shift in the nature of the Judith River fossil record can be explained by several accommodation-related factors. From a purely architectural perspective, the stacking and amalgamation of high-energy fluvial sandstones in the sub-discontinuity, low-accommodation McClelland Member would potentially destroy or disperse organic remains. A subsidence-related facies bias may have inhibited the concentration of vertebrate and invertebrate remains into readily discoverable bonebeds or shell beds in the sandstone-dominated lower Judith River Formation in the type area. Patterning in the Judith River fossil record may also reflect differential diagenesis and the impact of near-surface weathering on the long-term preservation of organic remains. The more intense weathering regime of the low-

accommodation phase may have selectively culled most bones and shells from the burial environment or at least degraded their quality, while the shift to high accommodation and accelerated aggradation presumably limited near-surface weathering while encouraging burial and eventual fossilization. Regardless of the exact mix of positive preservational parameters, there is no question that the shift to a relatively high-accommodation regimen in the Coal Ridge Member of the upper Judith River Formation created ideal conditions for fossil preservation.

## Conclusions

Stratigraphic analysis of the Judith River Formation in its type area confirms the presence of widespread shallow marine deposits both at the base of the Formation (Parkman Sandstone Member) and, more significantly, in its upper reaches. The new Woodhawk Member includes the distinctive shallow marine sandstones in the upper half of the formation in the eastern portion of the type area. These marine sandstones form a backstepping composite sequence set of three high-frequency sequences with cycle durations on the order of 0.3–0.4 Ma. Recognition of the Woodhawk Member advances understanding of regional geology in north-central Montana during the Campanian, especially in relation to sedimentation trends and shoreline stacking patterns during the early history of the Bearpaw transgression. New sanidine phenocryst $^{40}Ar/^{39}Ar$ ages from two bentonite beds positioned in the Judith River Formation at the approximate base of the Woodhawk Member indicate that transgression commenced ~76.2 Ma in north-central Montana. A new $^{40}Ar/^{39}Ar$ age from a bentonite ~5 m above the Woodhawk Member-Bearpaw Formation contact further indicates that sandy shorelines had advanced westward beyond north-central Montana by ~75.2 Ma.

The base of the Woodhawk Member correlates inland and updip with a pronounced break in the continuity of terrestrial sedimentation positioned approximately mid-unit in the Judith River Formation. This stratigraphic discontinuity is readily discernible in outcrop and can be traced in well logs for more than 27,000 $km^2$ beneath the plains of north-central Montana and southern Alberta and Saskatchewan. Terrestrial strata disposed on either side of the mid-Judith discontinuity are characterized by distinctive facies architecture, mineralogy, and fossil content. The new McClelland Ferry Member encompasses the sandstone-dominated suite of fluvial and floodplain strata below the discontinuity, whereas the new Coal Ridge Member encompasses the mudstone-dominated succession of alluvial strata above the discontinuity. These two new members can be distinguished in outcrop and subcrop throughout the type area and beyond. Their recognition promotes a more detailed regional perspective of previously undifferentiated terrestrial strata that represent most of the Judith River Formation.

New $^{40}Ar/^{39}Ar$ age data indicate that the mid-Judith discontinuity formed ~76.2 Ma, coincident with the onset of marine transgression. New age data, in combination with recalculated legacy ages, further indicate that rock accumulation rates more than doubled across the discontinuity, shifting from ~3.8 cm/1000 yr in the subjacent McClelland Ferry Member to ~9.0 cm/1000 yr in the superjacent Coal Ridge Member. With this shift from relatively low- to high-accommodation channel/floodplain ratios plummeted, channel sandstone thickness diminished significantly, and provenance of clastic detritus evolved as indicated by an increase in mafic volcanic clasts and plagioclase grains and the delivery of extraformational pebbles. The preservation potential of fossils in the Judith River Formation also increased dramatically, as reflected by the exceptionally rich fossil record in the Coal Ridge Member above the discontinuity.

Recognition of the mid-Judith discontinuity facilitates correlation and affords an outstanding opportunity to document the evolution of an alluvial depositional system during basin-scale geomorphic adjustment, which in this case corresponds with flexural subsidence and marine transgression. Correlation with the base of the Woodhawk Member indicates that the pulse of accommodation that drove transgression also forced major adjustments in the terrestrial realm that relate to key aspects of alluvial architecture, floodplain drainage and diagenesis, sediment sourcing, and fossil richness. Correlation with the base of the Woodhawk Member also helps contextualize the discontinuity in relation to sequence stratigraphy. The discontinuity is a major bounding surface, namely the proximal terrestrial extension of a maximum regressive surface, marking the shift from normal regression to transgression (fig. 2). The next step is to correlate more precisely between terrestrial and contemporaneous shallow marine deposits in order to determine how far key surfaces can be tracked inland (e.g., the flooding surfaces of the Woodhawk sequences). To this end, petrographic analyses targeting the abundant lignite beds in the Coal Ridge Member positioned landward of the Woodhawk Member are underway, with the goal of discerning maceral and mineral composition (e.g., Banerjee et al. 1996; Davies et al. 2006; Jerrett et al. 2011) in order

to better establish a high-frequency accommodation history in the terrestrial Judith River record.

## ACKNOWLEDGMENTS

We thank K. Curry Rogers, D. Eberth, B. Foreman, E. Hajek, S. Holland, and M. Patzkowsky for suggestions, observations, insights, and help with fieldwork and D. Eberth and E. Roberts for careful reviews of the manuscript and great suggestions. We also thank colleagues at the Bureau of Land Management (Lewistown Field Office, Billings State Office)—including Z. Fulbright, G. Liggett, C. Rye, G. Slagel, M. Schaefer, G. Smith, L. Anderson, J. Harkson, and L. Eichhorn—for their help over the years facilitating work in the Upper Missouri River Breaks National Monument. Friends in and around Winifred, Montana, are also acknowledged for their help and for allowing access to their land. Funding for this project was provided by the Petroleum Research Fund of the American Chemical Society, the National Science Foundation (EAR-1052673), the Bureau of Land Management, and Macalester College.

## REFERENCES CITED

Aitken, J. F., and Flint, S. S. 1995. The application of high-resolution sequence stratigraphy to fluvial systems: a case study from the Breathitt Group, eastern Kentucky, USA. Sedimentology 42:3–30.

Alexander, J., and Leeder, M. R. 1987. Active tectonic control on alluvial architecture. Spec. Publ. Soc. Econ. Paleontol. Mineral. 39:243–252.

Banerjee, I.; Kalkreuth, W.; and Davies, E. H. 1996. Coal seam splits and transgressive-regressive coal couplets: a key to stratigraphy of high frequency sequences. Geology 24:1001–1004.

Best, M. G.; Christiansen, E. H.; Deino, A. L.; Gromme, C. S.; and Tingey, D. G. 1995. Correlation and emplacement of a large, zoned, discontinuously exposed ash-flow sheet: $^{40}Ar/^{39}Ar$ chronology, paleomagnetism, and petrology of the Pahrangat Formation, Nevada. J. Geophys. Res. 100:24593–24609.

Birkeland, P. W. 1999. Soils and geomorphology. 3rd ed. New York, Oxford University Press, 448 p.

Bowen, C. F. 1915. The stratigraphy of the Montana group with special reference to the position and age of the Judith River formation in north-central Montana. U.S. Geol. Surv. Prof. Pap. 90:95–153.

———. 1920. Gradations from continental to marine conditions of deposition in central Montana during the Eagle and Judith River epochs. U.S. Geol. Surv. Prof. Pap. 125:11–21.

Bridge, J. S., and Leeder, M. R. 1979. A simulation model of alluvial stratigraphy. Sedimentology 26:617–644.

Brinkman, D. B. 1990. Paleoecology of the Judith River Formation (Campanian) of Dinosaur Provincial Park, Alberta, Canada: evidence from vertebrate microfossil localities. Palaeogeogr. Palaeoclimatol. Palaeoecol. 78: 37–54.

Case, G. R. 1978. A new selachian fauna from the Judith River Formation (Campanian) of Montana. Palaeontogr. Abt. A 160:176–205.

Catuneanu, O. 2006. Principles of sequence stratigraphy. Amsterdam, Elsevier, 375 p.

Catuneanu, O.; Galloway, W. E.; Kendall, C. G. St. C.; Miall, A. D.; Posamentier, H. W.; Strasser, A.; and Tucker, M. E. 2011. Sequence stratigraphy: methodology and nomenclature. Newsl. Stratigr. 44:173–245.

Catuneanu, O.; Miall, A. D.; and Sweet, A. R. 1997. Reciprocal architecture of Bearpaw T-R sequences, uppermost Cretaceous, Western Canada Sedimentary Basin. Bull. Can. Pet. Geol. 45:75–94.

Chamley, H. 1989. Clay sedimentology. Berlin, Springer, 623 p.

Clemens, W. A., and Goodwin, M. B. 1985. Vertebrate paleontology of the Judith River Formation, Montana. Res. Rep. Natl. Geogr. Soc. 21:71–78.

Clouse, V. R., and Horner, J. R. 1993. Eggs and embryos from the late Cretaceous Judith River Formation north central Montana. J. Vertebr. Paleontol. 13(suppl. 3): 31A.

Cohen, K. M.; Finney, S. C.; Gibbard, P. L.; and Fan, J.-X. 2013. The ICS international chronostratigraphic chart. Episodes 36:199–204.

Colombera, L.; Mountney, N. P.; and McCaffrey, W. D. 2015. A meta-study of relationships between channelbody stacking pattern and aggradation rate: implications for sequence stratigraphy. Geology 43:283–286.

Cope, E. D. 1871. Synopsis of the extinct Batrachia, Reptilia, and Aves of North America. Trans. Am. Philos. Soc. 14:1–252.

———. 1876. On some extinct reptiles and Batrachia from the Judith River and Fox Hills beds of Montana. Proc. Acad. Nat. Sci. Phila. 28:340–359.

———. 1877. Report on the geology of the region of the Judith River, Montana and on vertebrate fossils obtained on or near the Missouri River. Bull. U.S. Geol. Geogr. Surv. Terr. 3:565–597.

Davies, R.; Howell, J.; Boyd, R.; Flint, S.; and Diessel, C. 2006. High-resolution sequence-stratigraphic correlation between shallow-marine and terrestrial strata: examples from the Sunnyside Member of the Creta-

ceous Blackhawk Formation, Book Cliffs, eastern Utah. Am. Assoc. Pet. Geol. Bull. 90:1121–1140.

Dawson, G. M. 1875. Report on the geology and resources of the region in the vicinity of the forty-ninth parallel from the Lake of the Woods to the Rocky Mountains. Brit. N. Am. Bound. Comm., 379 p., pl. 1–18, 2 maps.

Dickinson, W. R. 1970. Interpreting detrital modes of graywacke and arkose. J. Sediment Petrol. 40:695–707.

Diehl, J. F.; Beck, M. E., Jr.; Beske-Diehl, S.; Jacobsen, D.; and Jearn, B. C., Jr. 1983. Paleomagnetism of the Late Cretaceous-Early Tertiary north-central Montana Alkalic Province. J. Geophys Res. 88:10593–10609.

Eberth, D. A. 1990. Stratigraphy and sedimentology of vertebrate microfossil sites in the uppermost Judith River Formation (Campanian), Dinosaur Provincial Park, Alberta, Canada. Palaeogeogr. Palaeoclimatol. Palaeoecol. 78:1–36.

———. 2005. The geology. *In* Currie, P. J., and Koppelhus, E. B., eds. Dinosaur Provincial Park: a spectacular ancient ecosystem revealed. Bloomington, Indiana University Press, p. 54–82.

Eberth, D. A., and Braman, D. R. 2012. A revised stratigraphy and depositional history for the Horseshoe Canyon Formation (Upper Cretaceous), southern Alberta Plains. Can. J. Earth Sci. 49:1053–1086.

Eberth, D. A.; Brinkman, D. B.; Chen, P.-J.; Yuan, F. T.; Wu, S.-Z.; Li, G.; and Cheng, X.-S. 2001. Sequence stratigraphy, paleoclimate patterns, and vertebrate fossil preservation in Jurassic-Cretaceous strata of the Junggar Basin, Xinjiang Autonomous Region, People's Republic of China. Can. J. Earth Sci. 38:1627–1644.

Eberth, D. A.; Evans, D. C.; Brinkman, D. B.; Therrien, F.; Tanke, D. H.; and Russell, L. S. 2013. Dinosaur biostratigraphy of the Edmonton Group (Upper Cretaceous), Alberta, Canada: evidence of climate influence. Can. J. Earth Sci. 50:701–726.

Eberth, D. A., and Hamblin, A. P. 1993. Tectonic, stratigraphic, and sedimentologic significance of a regional discontinuity in the upper Judith River Group (Belly River wedge) of southern Alberta, Saskatchewan, and northern Montana. Can. J. Earth Sci. 30:174–200.

Eberth, D. A.; Shannon, M.; and Noland, B. G. 2007. A bonebeds database: classification, biases and patterns of occurrence. *In* Rogers, R. R.; Eberth, D. A.; and Fiorillo, A. R., eds. Bonebeds: genesis, analysis, and paleobiological significance. Chicago, University of Chicago Press, p. 103–219.

Eberth, D. A.; Thomas, R. G.; and Deino, A. L. 1992. Preliminary K-Ar dates from bentonites in the Judith River and Bearpaw formations (Upper Cretaceous) at Dinosaur Provincial Park, southern Alberta, Canada. *In* Mateer, N. J., and Chen, P. J., eds. Aspects of nonmarine Cretaceous geology. Beijing, China Ocean, p. 296–304.

Eldridge, G. H. 1888. On some stratigraphical and structural features of the country about Denver, Colorado. Proc. Colo. Sci. Soc. 3:86–118.

———. 1889. Some suggestions upon the methods of grouping the formations of the middle Cretaceous and the employment of an additional term in its nomenclature. Am. J. Sci. 146:723–732.

Fiorillo, A. R. 1991. Taphonomy and depositional setting of Careless Creek Quarry (Judith River Formation), Wheatland County, Montana. U.S.A. Palaeogeogr. Palaeoclimatol. Palaeoecol. 81:281–311.

Fiorillo, A. R., and Currie, P. J. 1994. Theropod teeth from the Judith River Formation (Upper Cretaceous) of south-central Montana. J. Vertebr. Paleontol. 14:74–80.

Foreman, B. Z.; Rogers, R. R.; Deino, A. L.; Wirth, K. R.; and Thole, J. T. 2008. Geochemical characterization of bentonite beds in the Two Medicine Formation (Campanian, Montana), including a new $^{40}Ar/^{39}Ar$ age. Cretaceous Res. 29:373–385.

Fricke, H. C.; Rogers, R. R.; Backlund, R.; Dwyer, C. N.; and Echt, S. 2008. Preservation of primary stable isotope signals in dinosaur remains, and environmental gradients of the Late Cretaceous of Montana and Alberta. Palaeogeogr. Palaeoclimatol. Palaeoecol. 266:13–27.

Fricke, H. C.; Rogers, R. R.; and Gates, T. A. 2009. Hadrosaurid migration: inferences based on stable isotope comparisons among Late Cretaceous dinosaur localities. Paleobiology 35:270–288.

Fuentes, F.; DeCelles, P. G.; Constenuis, K. N.; and Gehrels, G. E. 2011. Evolution of the Cordilleran foreland basin system in northwestern Montana, U.S.A. Geol. Soc. Am. Bull. 123:507–533.

Gill, J. R., and Cobban, W. A. 1973. Stratigraphy and geologic history of the Montana group and equivalent rocks, Montana, Wyoming, and North and South Dakota. U.S. Geol. Surv. Prof. Pap. 776, 37 p.

Goodwin, M. B., and Deino, A. L. 1989. The first radiometric ages from the Judith River Formation (Late Cretaceous), Hill County, Montana. Can. J. Earth Sci. 26:1384–1391.

Hajek, E. A., and Heller, P. L. 2012. Flow-depth scaling in alluvial architecture and nonmarine sequence stratigraphy: example from the Castlegate Sandstone, central Utah, U.S.A. J. Sediment Res. 82:121–130.

Hajek, E. A.; Heller, P. L.; and Schur, E. L. 2012. Field test of autogenic control on alluvial stratigraphy (Ferris Formation, Upper Cretaceous–Paleogene, Wyoming). Geol. Soc. Am. Bull. 124:1898–1912.

Hamblin, A. P., and Abramson, B. W. 1996. Stratigraphic architecture of "basal Belly River" cycles, Foremost Formation, Belly River Group, subsurface of southern Alberta and southwestern Saskatchewan. Bull. Can. Pet. Geol. 44:654–673.

Hatcher, J. B. 1903*a*. The Judith River beds. Science 17:471–472.

———. 1903*b*. Relative age of the Lance Creek (Ceratops) beds of Converse County, Wyoming, the Judith River beds of Montana, and the Belly River beds of Canada. Am. Geol. 31:369–375.

Hatcher, J. B., and Stanton, T. W. 1903. The stratigraphic position of the Judith River beds and their correlation with the Belly River beds. Science 18:211–212.

Hayden, F. V. 1857. Notes explanatory of a map and section illustrating the geologic structure of the country bordering the Missouri River from the mouth of the Platte River to Fort Benton. Proc. Acad. Nat. Sci. Phila. 9:109–116.

———. 1871. Geology of the Missouri River Valley. U.S. Geol. Surv. Terr. (Fourth Annual). Preliminary Rep., pt. 2, chap. 7, p. 85–98.

Helland-Hansen, W., and Gjelberg, J. G. 1994. Conceptual basis and variability in sequence stratigraphy: a different perspective. Sediment. Geol. 92:31–52.

Helland-Hansen, W., and Martinsen, O. J. 1996. Shoreline trajectories and sequences: description of variable depositional-dip scenarios. J. Sediment Res. 66: 670–688.

Hillier, S. 2003. Quantitative analysis of clay and other minerals in sandstones by X-ray powder diffraction (XRPD). *In* Worden, R. H., and Morad, S., eds. Clay mineral cements in sandstones. Spec. Publ. Int. Assoc. Sediment. 34:213–251.

Holbrook, J. M., and Bhattacharya, J. P. 2012. Reappraisal of the sequence boundary in time and space: case and considerations for an SU (subaerial unconformity) that is not a sediment bypass surface, a time barrier, or an unconformity. Earth-Sci. Rev. 113: 271–302.

Horner, J. R. 1988. A new hadrosaur (Reptilia: Ornithischia) from the Upper Cretaceous Judith River Formation of Montana. J. Vertebr. Paleontol. 8:314–321.

———. 1999. Egg clutches and embryos of two hadrosaurian dinosaurs. J. Vertebr. Paleontol. 19:607–611.

Huggett, J. M. 1986. An SEM study of phyllosilicate diagenesis in sandstones and mudstones in the Westphalian Coal Measures using back-scattered electron microscopy. Clay Miner. 21:603–616.

Jerrett, R. M.; Flint, S. S.; Davies, R. C.; and Hodgson, D. M. 2011. Sequence stratigraphic interpretation of a Pennsylvanian (Upper Carboniferous) coal from the central Appalachian Basin, USA. Sedimentology 58:1180–1207.

Jerzykiewicz, T., and Norris, D. K. 1994. Stratigraphy, structure and syntectonic sedimentation of the Campanian "Belly River" clastic wedge in the southern Canadian Cordillera. Cretaceous Res. 15:367–399.

Jinnah, Z. A.; Roberts, E. M.; Deino, A. L.; Larsen, J. S.; Link, P. K.; and Fanning, C. M. 2009. New $^{40}Ar$-$^{39}Ar$ and detrital zircon U-Pb ages for the Upper Cretaceous Wahweap and Kaiparowits formations on the Kaiparowits Plateau, Utah: implications for regional correlation, provenance, and biostratigraphy. Cretaceous Res. 30:287–299.

John, C. M. 2004. Plotting and analyzing data trends in ternary diagrams made easy. Eos 85:158.

Kauffman, E. G. 1977. Geological and biological overview: Western Interior Cretaceous basin. Mountain Geol. 14:75–99.

Ketzer, J. M.; Morad, S.; and Amorosi. A. 2003. Predictive diagenetic clay-mineral distribution in siliciclastic rocks within a sequence stratigraphic framework. *In* Worden, R. H., and Morad, S., eds. Clay mineral cements in sandstones. Spec. Publ. Int. Assoc. Sediment. 34:43–61.

Khidir, A., and Catuneanu, O. 2009. Predictive diagenetic clay-mineral distribution in siliciclastic rocks as a tool for identifying sequence boundaries in nonmarine successions: the Coalspur Formation, west-central Alberta. Geologos 15:169–180.

Kidwell, S. M. 1988. Taphonomic comparison of passive and active continental margins: Neogene shell beds of the Atlantic coastal plain and Northern Gulf of California. Palaeogeogr. Palaeoclimatol. Palaeoecol. 63:201–223.

———. 1993*a*. Influence of subsidence on the anatomy of marine siliciclastic sequences and on the distribution of shell and bone beds. J. Geol. Soc. Lond. 150:165–167.

———. 1993*b*. Taphonomic expressions of sedimentary hiatuses: field observations on bioclastic concentrations and sequence anatomy in low, moderate and high subsidence settings. Geol. Rundsch. 82:189–202.

Klug, B. 1993. Cyclic facies architecture as a key to depositional controls in a distal foredeep: Campanian Mesaverde Group, Wyoming, USA. Geol. Rundsch. 82:306–326.

Knechtel, M. M., and Patterson, S. H. 1956. Bentonite deposits in marine Cretaceous formations of the Hardin district, Montana and Wyoming. U.S. Geol. Surv. Bull. 1023, 116 p.

Knowlton, F. H. 1911. Remarks on the fossil turtles accredited to the Judith River Formation. Proc. Wash. Acad. Sci. 13:51–65.

Kuiper, K. F.; Deino, A.; Hilgen, F. J.; Krijgsman, W.; Renne, P. R.; and Wijbrans, J. R. 2008. Synchronizing the rock clocks of Earth history. Science 320: 500–504.

Lambe, L. M. 1907. On a new crocodilian genus and species from the Judith River Formation of Alberta. Trans. R. Soc. Can. 3:219–244.

Lawton, T. F. 1986. Fluvial systems of the Upper Cretaceous Mesaverde Formation, Central Utah: a record of transition from thin-skinned to thick-skinned deformation in the foreland region. *In* Peterson, J. A., ed. Paleotectonics and sedimentation in the Rocky Mountain region. Am. Assoc. Pet. Geol. Mem. 41: 423–442.

Leckie, D. A., and Boyd, R. 2003. Towards a nonmarine sequence stratigraphic model. Salt Lake City, UT, Am. Assoc. Pet. Geol. Annual Convention, Official Program 12:A101.

Lee, J.-Y.; Marti, K.; Severinghaus, J. P.; Kawamura, K.; Yoo, H.-S.; Lee, J. B.; and Kim, J. S. 2006. A redetermination of the isotopic abundances of atmospheric Ar. Geochim. Cosmochim. Acta 70:4507–4512.

Leeder, M. R. 1978. A quantitative stratigraphic model for alluvium, with special reference to channel de-

posit density and interconnectedness. Mem. Can. Soc. Pet. Geol. 5:587–596.

Leidy, J. 1856. Notices of the remains of extinct reptiles and fishes discovered by Dr. F. V. Hayden in the badlands of the Judith River, Nebraska Territory. Proc. Acad. Nat. Sci. Phila. 8:72–73.

———. 1860. Extinct vertebrata from the Judith River and Great Lignite formations of Nebraska. Trans. Am. Philos. Soc. 11:139–154.

Lindvall, R. M., 1962. Geology of the Eskay Quadrangle, Chouteau and Blaine Counties, Montana. U.S. Geol. Surv. Misc. Geol. Invest. Map I-353.

Lorenz, J. C. 1981. Sedimentary and tectonic history of the Two Medicine Formation, Late Cretaceous (Campanian), northwestern Montana. PhD dissertation, Princeton University, Princeton, NJ.

McBride, E. F. 1963. A classification of common sandstones. J. Sediment. Petrol. 33:664–669.

McCarthy, P. J.; Faccini, U. F.; and Plint, A. G. 1999. Evolution of an ancient coastal plain: paleosols, interfluves and alluvial architecture in a sequence stratigraphic framework, Cenomanian Dunvegan Formation, NE British Columbia, Canada. Sedimentology 46:861–891.

McKay, J. L.; Longstaffe, F. J.; and Plint, A. G. 1995. Early diagenesis and its relationship to depositional environment and relative sea-level fluctuations (Upper Cretaceous Marshybank Formation, Alberta and British Columbia). Sedimentology 42:161–190.

McLean, J. R. 1971. Stratigraphy of the Upper Cretaceous Judith River Formation in the Canadian Great Plains. Sask. Res. Counc. Geol. Div. Rep. 11, 97 p.

Meek, F. B. 1876. A report on the invertebrate Cretaceous and Tertiary fossils of the upper Missouri country. Rep. U.S. Geog. Surv. Terr. 9, 629 p.

Meek, F. B., and Hayden, F. V. 1856. Descriptions of a new species of Acephala and Gastropoda from the Tertiary formations of Nebraska Territory, with some general remarks on the geology of the country about the sources of the Missouri River. Proc. Acad. Nat. Sci. Phila. 8:111–126.

———. 1857. Descriptions of new species and genera of fossils, collected by Dr. F. V. Hayden in Nebraska Territory; with some remarks on the Tertiary and Cretaceous formations of the northwest. Proc. Acad. Nat. Sci. Phila. 9:117–148.

Miall, A. D. 1997. The geology of stratigraphic sequences. Berlin, Springer, 433 p.

Miall, A. D., and Arush, M. 2001. Cryptic sequence boundaries in braided fluvial successions. Sedimentology 48:971–985.

Min, K.; Mundil, R.; Renne, P. R.; and Ludwig, K. R. 2000 A test for systematic errors in $^{40}Ar/^{39}Ar$ geochronology through comparison with U/Pb analysis of a 1.1-Ga rhyolite. Geochim. Cosmochim. Acta. 64:73–96.

Mitchum, R. M., and Van Wagoner, J. C. 1991. High-frequency sequences and their stacking patterns: sequence-stratigraphic evidence of high-frequency eustatic cycles. Sediment. Geol. 70:131–160.

Montellano, M. 1991. Mammalian fauna of the Judith River Formation (Late Cretaceous, Judithian) north central Montana. Univ. Calif. Publ. Geol. Sci. 136, 115 p.

North American Code on Stratigraphic Nomenclature. 2005. North American stratigraphic code. Am. Assoc. Pet. Geol. Bull. 89:1547–1591.

Ogg, J. G., and Hinnov, L. A. 2012. Chapter 27: Cretaceous. *In* Gradstein, F. M.; Ogg, J. G.; Schmitz, M. D.; and Ogg, G. M., eds. The geological time scale. Elsevier, Amsterdam, p. 793–853.

Ostrom, J. H. 1964. The systematic position of *Hadrosaurus* (*Ceratops*) *paucidens* Marsh. J. Paleontol. 38: 130–134.

Payenberg, T. H. D.; Braman, D. R.; and Miall, A. D. 2003. Depositional environments and stratigraphic architecture of the Late Cretaceous Milk River and Eagle formations, southern Alberta and north-central Montana: relationships to shallow biogenic gas. Bull. Can. Petrol. Geol. 51:155–176.

Peale, A. C. 1912. On the stratigraphic position and age of the Judith River Formation. J. Geol. 20:530–549.

Phillips, D., and Matchan, E. L. 2013. Ultra-high precision $^{40}Ar/^{39}Ar$ ages for Fish Canyon Tuff and Alder Creek Rhyolite sanidine: new dating standards required? Geochim. Cosmochim. Acta 121:229–239.

Plint, A. G.; McCarthy, P. J.; and Faccini, U. 2001. Nonmarine sequence stratigraphy: updip expression of sequence boundaries and systems tracts in a high-resolution framework, Cenomanian Dunvegan Formation, Alberta foreland basin, Canada. Am. Assoc. Pet. Geol. Bull. 85:1967–2001.

Posamentier, H. W., and Vail, P. R. 1988. Eustatic controls on clastic deposition. II. Sequence and systems tract models. *In* Wilgus, C. K.; Hastings, B. S.; Kendall, C. G. St. C.; Posamentier, H. W.; Ross, C. A.; and Van Wagoner, J. C., eds. Sea level changes: an integrated approach. SEPM Spec. Publ. 42:125–154.

Prieto-Marquez, A. 2005. New information on the cranium of *Brachylophosaurus canadensis* (Dinosauria, Hadrosauridae); with a revision of its phylogenetic position. J. Vertebr. Paleontol. 25:144–156.

Renne, P. R. 2013. Some footnotes to the optimization-based calibrations of the $^{40}Ar/^{39}Ar$ system. *In* Jourdan, F.; Mark, D. F.; and Verati, C., eds. Advances in $^{40}Ar/^{39}Ar$ dating: from archaeology to planetary sciences. Geol. Soc. Lond. Spec. Pub. 378:21–31.

Roberts, E. M.; Deino, A. L.; and Chan, M. A. 2005. $^{40}Ar/^{39}Ar$ age of the Kaiparowits Formation, southern Utah, and correlation of contemporaneous Campanian strata and vertebrate faunas along the margin of the Western Interior Basin. Cretaceous Res. 26:307–318.

Roberts, E. M., and Hendrix, M. S. 2000. Taphonomy of a petrified forest in the Two Medicine Formation (Campanian), northwest Montana: implications for palinspastic restoration of the Boulder Batholith and Elkhorn Mountains Volcanics. Palaios 15:476–482.

Roberts, E. M.; Sampson, S. D.; Deino, A. L.; Bowring, S. A.; and Buchwaldt, R. 2013. The Kapairowits Formation: a remarkable record of Late Cretaceous environments, ecosystems, and evolution in western North America. *In* Titus, A. L., and Loewen, M. E., eds. At the top of the grand staircase: the Late Cretaceous of southern Utah. Bloomington, Indiana University Press, p. 85–106.

Rogers, R. R. 1993. Systematic patterns of time averaging in the terrestrial vertebrate record: a Cretaceous case study. *In* Kidwell, S. K., and Behrensmeyer, A. K., eds. Taphonomic approaches to time resolution in fossil assemblages. Short Course Paleontol. 6:228–249.

———. 1994. Nature and origin of through-going discontinuities in nonmarine foreland basin deposits, Upper Cretaceous, Montana: implications for sequence analysis. Geology 22:1119–1122.

———. 1995. Sequence stratigraphy and vertebrate taphonomy of the Upper Cretaceous Two Medicine and Judith River Formations, Montana. PhD dissertation, University of Chicago.

———. 1998. Sequence analysis of the upper Cretaceous Two Medicine and Judith River formations, Montana: nonmarine response to the Claggett and Bearpaw marine cycles. J. Sediment Res. 68:615–631.

Rogers, R. R., and Brady, M. E. 2010. Origins of microfossil bonebeds: insights from the Upper Cretaceous Judith River Formation of north-central Montana. Paleobiology 36:80–112.

Rogers, R. R.; Fricke, H. C.; Addona, V.; Canavan, R. R.; Dwyer, C. N.; Harwood, C. L.; Koenig, A. E.; Murray, R.; Thole, J. T.; and Williams, J. 2010. Using laser ablation–inductively coupled plasma–mass spectrometry (LA-ICP-MS) to explore geochemical taphonomy of vertebrate fossils in the Upper Cretaceous Two Medicine and Judith River Formations of Montana. Palaios 25:183–195.

Rogers, R. R., and Kidwell, S. M. 2000. Associations of vertebrate skeletal concentrations and discontinuity surfaces in terrestrial and shallow marine records: a test in the Cretaceous of Montana. J. Geol. 108:131–154.

Rogers, R. R.; Swisher, C. C.; and Horner, J. R. 1993. $^{40}Ar/^{39}Ar$ age and correlation of the non-marine Two Medicine Formation (Upper Cretaceous), northwestern Montana: Can. J. Earth Sci. 30:1066–1075.

Ryan, M. J.; Evans, D. C.; Currie, P. J.; and Loewen, M. A. 2014. A new chasmosaurine from northern Laramidia expands frill disparity in ceratopsid dinosaurs. Naturwissenschaften 101:505–512.

Sahni, A. 1972. The vertebrate fauna of the Judith River Formation, Montana. Bull. Am. Mus. Nat. Hist. 147: 321–412.

Schott, R. K.; Evans, D. C.; Williamson, T. E.; Carr, T. D.; and Goodwin, M. B. 2010. The anatomy and systematics of *Colepiocephale lambei* (Dinosauria: Pachycephalosauridae). J. Vertebr. Paleontol. 29:771–786.

Sears, J. W. 2001. Emplacement and denudation history of the Lewis-Eldorado-Hoadley thrust slab in the northern Montana Cordillera, USA: implications for steady-state orogeny processes. Am. J. Sci. 301: 359–373.

Smedes, H. W. 1966. Geology and igneous petrology of the northern Elkhorn mountains, Jefferson and Broadwater counties, Montana. U.S. Geol. Surv. Prof. Pap. 510.

Stanton, T. W., and Hatcher, J. B. 1903. The stratigraphic position of the Judith River beds and their correlation with the Belly River beds. Science 16: 1031–1032.

———. 1905. Geology and paleontology of the Judith River beds. U.S. Geol. Surv. Bull. 257:1–128.

Stebinger, E. 1914. The Montana Group of northwestern Montana. U.S. Geol. Surv. Prof. Pap. 90-G:60–68.

Sternberg, C. H. 1914. Notes on the fossil vertebrates collected on the Cope expedition to the Judith River and Cow Island beds, Montana, in 1876. Science 40:134–135.

Taylor, K. G., and Gawthorpe, R. L. 2003. Basin-scale dolomite cementation of shoreface sandstones in response to sea level fall. Geol. Soc. Am. Bull. 115: 1218–1229.

Taylor, K. G.; Gawthorpe, R. L.; and Van Wagoner, J. C. 1995. Stratigraphic control on laterally persistent cementation, Book Cliffs, Utah. J. Geol. Soc. Lond. 152:225–228.

Taylor, K. G., and Machent, P. G. 2010. Systematic sequence-scale controls on carbonate cementation in a siliciclastic sedimentary basin: examples from Upper Cretaceous shallow marine deposits of Utah and Colorado, USA. Mar. Petrol. Geol. 27:1297–1310.

Tedesco, A.; Cicciolo, P.; Suriano, J.; and Limarino, C. O. 2010. Changes in the architecture of fluvial deposits in the Paganzo Basin (Upper Paleozoic of San Juan Province): an example of sea level and climatic controls on the development of coastal fluvial environments. Geol. Acta 8:463–482.

Thomas, R. G.; Eberth, D. A.; Deino, A. L.; and Robinson, D. 1990. Composition, radioisotopic ages, and potential significance of an altered volcanic ash (bentonite) from the Upper Cretaceous Judith River Formation, Dinosaur Provincial Park, southern Alberta, Canada. Cretaceous Res. 11:126–162.

Tilling, R. I.; Klepper, M. R.; and Obradovich, J. D. 1968. K-Ar ages and time span of emplacement of the Boulder Batholith, Montana. Am. J. Sci. 266:671–689.

Tschudy, B. D. 1973. Palynology of the Upper Campanian (Cretaceous) Judith River Formation, north-central Montana. U.S. Geol. Surv. Prof. Pap. 770, 42 p.

Tweet, J. S.; Chin, K.; Bramen, D. R.; and Murphy, N. L. 2008. Probable gut contents within a specimen of *Brachylophosaurus canadensis* (Dinosauria, Hadrosauridae) from the Upper Cretaceous Judith River Formation of Montana. Palaios 23:624–635.

Viele, G. W., and Harris, F. G. II. 1965. Montana Group stratigraphy, Lewis and Clark County, Montana. Am. Assoc. Pet. Geol. Bull. 39:379–417.

Waage, K. M. 1975. Deciphering the basic sedimentary structure of the Cretaceous System in the Western Interior. Geol. Assoc. Can. Spec. Pap. 13:55–81.

Weimer, R. J. 1960. Upper Cretaceous stratigraphy, Rocky Mountain area. Am. Assoc. Pet. Geol. Bull. 44:1–20.

———. 1963. Stratigraphy of the upper Judith River Formation (Late Cretaceous), central and southeast Montana. Wyoming Geol. Assoc. Billings Geol. Soc. 1963 Joint Field Conf., p. 108–111.

Wood, J. M. 1989. Alluvial architecture of the Upper Cretaceous Judith River Formation, Dinosaur Provincial Park, Alberta, Canada. Bull. Can. Petrol. Geol. 37:169–181.

Wood, J. M.; Thomas, R. G.; and Visser, J. 1988. Fluvial processes and vertebrate taphonomy: the Upper Cretaceous Judith River Formation, south central Dinosaur Provincial Park, Alberta, Canada. Palaeogeogr. Palaeoclimatol. Palaeoecol. 66:127–143.

Wright, V. P., and Marriott, S. B. 1993. The sequence stratigraphy of fluvial depositional systems: the role of floodplain sediment storage. Sediment. Geol. 86:203–210.